PK ISSN 0022- 2941; CODEN JNSMAC
Vol. 46, No.1 & 2 (April & October 2006) PP 1-11

A SYSTEM OF LINEAR QUATERNION MATRIX EQUATIONS WITH APPLICATIONS

CHUN-YAN LIN
School of Statistics and Sciences, Shandong Finance University
40 Shungeng Road, 250014, Jinan, P.R. China
E-mail: 1.chy@163.com

(Received: January 1,2006)

ABSTRACT: The general solution of the system of quaternion matrix equations

$$A_1X = C_1, XB_2 = C_2, A_3X = C_3, XB_4 = C_4$$

is considered. A necessary and sufficient, condition for the existence and for the representation of the general solution of such a system is given. As applications, necessary and sufficient conditions for the existence and the expressions of the bisymmetric solutions for the matrix equation $XB = C$; is given centrosymmetric solution of

$$\begin{cases} A_1X = C_1 \\ XB_2 = C_2 \end{cases}$$

and the persymmetric solution to

$$\begin{cases} A_1X = C_1 \\ A_3X = C_3 \end{cases}$$

are given, respectively, Moreover 1 some auxiliary results on other systems of quaternion matrix equations are also mentioned.

Keywords: System of linear quaternion matrix equations; reflexive inverse of a matrix; bisymmetric matrix; centrosymmetric, persymmetric matrix
2000 AMS Subject Classifications 15A24, 15A33, 15A57, 15A09

1. INTRODUCTION

In 1976, Khatri and Mitra [1] have studied the Hermitian solutions to the following matrix equations over the complex field

$$AX = C \tag{1.1}$$

and

$$\begin{cases} A_1X = C_1 \\ XB_2 = C_2 \end{cases} \tag{1.2}$$

The inverse problem of the matrix equation (1.1), i.e. the matrix equation

1Supported by PhD Foundation of Shandong Finance University

$$XB = C \tag{1.3}$$

has been investigated in [2]-[4]. The symmetric solution and Hermitian solutions for (1.1) have been investigated by many authors, e.g. Vetter [5], Magnus and Neudecker [6], Don [8], and Dai [9]. Mitra in [10] presented further investigation for the system (1.2). Chu [7] studied the symmetric solutions of the system of linear real matrix equations.

$$\begin{cases} A_1 X = C_1 \\ A_3 X = C_3 \end{cases} \tag{1.4}$$

Controsymmetric, persymmetric and bisymmetric matrices have been widely discussed (e.g [11]-[12]), which are very useful in various physics and engineering problems [12], in the study of some markov processes [14], in the numerical solution of certain differential equations, information theory, linear system theory, linear estimation theory [13], and others.

Motivated by the work mentioned above, we consider the following system

$$\begin{cases} A_1 X = C_1 \\ XB_2 = C_2 \\ A_3 X = C_3 \\ XB_4 = C_4 \end{cases} \tag{1.5}$$

over the real quaternion field H. In section 2, we derive a necessary and sufficient condition for the existence and representation of the general solution for the system (1.5). Moreover 1 as special cases, the corresponding results on the systems (1.4) and

$$\begin{cases} XB_2 = C_2 \\ XB_4 = C_4 \end{cases} \tag{1.6}$$

over H are also given. In section 3, as applications of Section 2, we present necessary and sufficient conditions for the existence of bisymmetric solution for the matrix equation (1.3), persymmetric solution of the systems (1.4), centrosymmetric solution for the system (1.2) over H; and give expression of such solutions when the corresponding conditions hold.

Throughout this we denote the set of all $m \times n$ matrices over H by $\mathrm{H}^{m \times n}$, the identity matrix with appropriate sizes by I, a reflexive inverse of a matrix A over H by A^+. This last one satisfies simultaneously $AA^+A = A$ and $A^+AA^+ = A^+$. Moreover, $L_A = I - A^+A$, $R_A = I - AA^+$ where A^+ is any but fixed.

2. THE GENERAL SOUTION TO THE SYSTEM (1.5) OVER H

In this section we consider the system (1.5) over H.

Lemma 2.1. (Lemma 2.2 in [23]) Let $A \in H^{m\times n}, B \in H^{r\times s}$ *and* $C \in H^{m\times s}$. **Then the following condition are equivalent:**

(1) The matrix equation

$$A X B = C \tag{2.1}$$

is consistent.

(2) $AA^{+}CB^{+}B = C.$

(3) $CL_B = 0, R_A C = 0$

In that case, the general solution of (2.1) can be expressed as

$$X = A^{+} CB^{+} + L_A V + UR_B \tag{2.2}$$

where U **and** V **are any matrices with compatible dimensions over** H.

Lemma 2.2 Let $A_1 \in H^{m\times n}, B_2 \in H^{r\times s}, C_1 \in H^{m\times r}, C_2 \in H^{n\times s}$ **be known and** $X \in H^{n\times r}$ **unknown. Then the system (1.2) is consistent if and only if**

$$A_1 A_1^{+} C_1 = C_1, C_2 B_2^{+} B_2 = C_2, A_1 C_2 = C_1 B_2 \tag{2.3}$$

in that case, the general solution of the system (1.2) is

$$X = A_1^{+} C_1 + L_{A_1} C_2 B_2^{+} + L_{A_1} Y R_{B_2}. \tag{2.4}$$

where Y **is an arbitrary matrix over** H **with appropriate dimensions. Now we give the main result of this paper.**

Theorem 2.3: Let $A_1 \in H^{m\times n}, A_3 \in H^{k\times n}, B_2 \in H^{r\times s}, B_4 \in H^{r\times l}, C_1 \in H^{m\times r}, C_2 \in H^{n\times s}, C_3 \in H^{k\times r}, C_4 \in H^{n\times l}$ **be known matrices and** $X \in H^{n\times r}$ **unknown; and** $K = A_3 L_{A_1}, M = L_{A_1} L_K, N = R_{B_2} B_4,$

$$T = C_3 - A_3 A_1^{+} C_1, Q_1 = T - K C_2 B_2^{+}, \tag{2.5}$$

$$Q = C_4 - A_1^{+} C_1 B_4 - L_{A_1} C_2 B_2^{+} B_4 - L_{A_1} K^{+} TN. \tag{2.6}$$

Then the system (1.5) is consistent if and only if

$$KK^{+} TR_{B_2} = Q_1 Q L_N = 0, R_M Q = 0, \tag{2.7}$$

$$A_i A_i^{+} C_i, i = 1,3, A_1 C_2 = C_1 B_2, C_j B_j^{+} B_j = C_j, j = 2,4 \tag{2.8}$$

In this case, the general solution of (1.5) can be expressed as the following:

$$X = A_1^{+} C_1 + L_{A_1} C_2 B_2^{+} + L_{A_1} K^{+} TR_{B_2} + QN + R_{B_2} + MZR_N R_{B_2} \tag{2.9}$$

where Z **is an arbitrary matrix over** H **with compatible dimensions.**

Proof. The Proof consists of two main parts. We first show that the matrix X **that has the form of (2.9) is a solution of the system (1.5) under the**

assumption (2.7) and (2.8), then prove that any solution of the system (1.5) can be expressed as the form of (2.9), when (2.7) and (2.8) hold.

Suppose that (2.7) and (2.8) hold. Noting that $A_1L_{A_1} = 0,\ MM^+Q = Q$**, we can easily verify that the matrix** X **that has the form of (2.9) is a solution of the equation** $A_1X = C_1$**. It follows from (2.8) and** $R_{B_2}B_2 = 0$ **that** $XB_2 = 0.$ **Note that** $A_3M = A_3L_{A_1}L_K = KL_K = 0.$ **So** $MM^+Q = Q$ **yields** $A_3Q = 0$**. Hence by (2.5) and the first equation of (2.7), we have the following**

$$A_3X = A_3A_1^+C_1 + KC_2B_2^+ + Q_1 = C_3.$$

Now we prove that $XB_4 = C_4$**. By** $R_NN = 0, QN^+N = Q$ **and (2.6), we have**

$$\begin{aligned} XB_4 &= A_1^+C_1B_4 + L_{A_1}C_2B_2^+B_4 + L_{A_1}K^+TN + Q \\ &= C_4 \end{aligned}$$

To sum up, a matrix X **that has the form of (2.9) is a solution of the system (1.5) under the assumptions (2.7) and (2.8).**

Conversely, assume that the system (1.5) has a solution X_0**, then** X_0 **is a solution of the system (1.2) and** $A_3X_0 = C_3, X_0B_4 = C_4$**. By Lemma 2.2 and Lemma 2.1, (2.8) holds and**

$$X_0 = A_1^+C_1 + L_{A_1}C_2B_2^+ + L_{A_1}YR_{B_2}. \qquad \textbf{(2.10)}$$

So

$$C_3 = A_3X_0 = A_3(A_1^+C_1 + L_{A_1}C_2B_2^+ + L_{A_1}YR_{B_2}),$$

i.e., the matrix equation $KYR_{B_2} = Q_1$ **is consistent for** Y **where** Q_1 **is defined by (2.5). Note that** R_{B_2} **is idempotent and a reflexive inverse of** R_{B_2} **is itself and** $R_{R_{B_2}} = I - R_{B_2}$**. Hence it follows from Lemma 2.1 that the first equation of (2.7) holds and**

$$Y = K^+Q_1R_{B_2} + L_KV + U(I - R_{B_2})$$

where U **and** V **are arbitrary matrices with appropriate sizes over** H**. Therefore** $B_2^+R_{B_2} = 0$ **and (2.5), (2.10) becomes**

$$X_0 = A_1^+C_1 + L_{A_1}C_2B_2^+ + L_{A_1}K^+TR_{B_2} + L_{A_1}L_KVR_{B_2}.$$

Hence by (2.6), (2.5) and $C_4 = X_0B_4$**, we have the fact that**

$$MVN = Q.$$

So Lemma 2.1 yields the later two equations of (2.7).
Now we show that X_0 can be expressed as the form of (2.9). It follows from $L_{A_1} X_0 = X_0 - A_1^+ C_1$ that

$$\begin{aligned} L_K X_0 R_{B_2} &= X_0 R_{B_2} - K^+ K X_0 R_{B_2} \\ &= X_0 - X_0 B_2 B_2^+ - K^+ K X_0 R_{B_2} \\ &= X_0 - C_2 B_2^+ - K^+ A_3 L_{A_1} X_0 R_{B_2} \\ &= X_0 - C_2 B_2^+ - K + C_3 R_{B_2} + K^+ A_3 A_1^+ C_1 R_{B_2} \end{aligned}$$

Therefore by (2.5), we have the following

$$\begin{aligned} L_{A_1} L_K X_0 R_{B_2} &= X_0 - A_1^+ C_1 - L_{A_1} C_2 B_2^+ - L_{A_1} K^+ C_3 R_{B_2} + L_{A_1} K^+ A_3 A_1 + C_1 R_{B_2} \\ &= X_0 - A_1^+ C_1 - L_{A_1} C_2 B_2^+ - L_{A_1} K^+ T R_{B_2} \end{aligned}$$

whence in view of (2.6),

$$\begin{aligned} L_{A_1} L_K X_0 N N^+ R_{B_2} &= L_{A_1} L_K X_0 R_{B_2} B_4 N^+ R_{B2} \\ &= (X_0 - A_1^+ C_1 - L_{A_1} C_2 B_2^+ - L_{A_1} K^+ T R_{B_2}) B_4 N^+ R_{B_2} \\ &= (C_4 - A_1^+ C_1 B_4 - L_{A_1} C_2 B_2^+ B_4 - L_{A_1} K^+ T N) N^+ R_{B_2} \\ &= Q N^+ R_{B_2}. \end{aligned}$$

Hence

$$\begin{aligned} M X_0 R_N R_{B_2} &= L_{A_1} L_K X_0 R_N R_{B_2} \\ &= L_{A_1} L_K X_0 R_{B_2} - L_{A_1} L_K X_0 N N^+ R_{B_2} \\ &= X_0 - A_1^+ C_1 - L_{A_1} C_2 B_2^+ - L_{A_1} K^+ T R_{B_2} - Q N^+ R_{B_2}, \end{aligned}$$

i.e.

$$X_0 = A_1^+ C_1 + L_{A_1} C_2 B_2^+ + L_{A_1} K^+ T R_{B_2} + Q N^+ R_{B_2} + M X_0 R_N R_{B_2}.$$

So X_0 can be expressed as the form of (2.9) where $Z = X_0$.

In Theorem 2.3, let B_2, B_4, C_2 and C_4 vanish. Then we have the following.

Corollary 2.4 Let $A_1 \in \mathrm{H}^{m\times n}, A_3 \in \mathrm{H}^{k\times n}, C_1 \in \mathrm{H}^{m\times r}, C_3 \in \mathrm{H}^{k\times r}$ **be known matrices and** $X \in \mathrm{H}^{n\times r}$ **unknown; and** $\mathrm{K} = A_3 L_{A_1}, T = C_3 - A_3 A_1^{+} C_1$**. Then the system (1.4) is consistent if and only if.**

$$KK^{+}T = T, A_i A_i^{+} C_i = C_i, i = 1,3,$$

in which case, the general solution of (1.4) can be expressed as the following:

$$X = A_1^{+} C_1 + L_{A_1} K^{+} T + L_{A_1} L_K Z$$

where Z **is an arbitrary matrix over** H **with compatible dimensions.**

In Theorem 2.3, let A_1, C_1, A_3 **and** C_3 **vanish. Then we have the following.**

Corollary 2.5. Let $B_2 \in \mathrm{H}^{r\times s}, B_4 \in \mathrm{H}^{r\times l}, C_2 \in \mathrm{H}^{n\times s}, C_4 \in \mathrm{H}^{n\times l}$ **known matrices and** $X \in \mathrm{H}^{n\times r}$ **unknown; and** $N = R_{B_2} B_4, Q = C_4 - C_2 B_2^{+} B_4$**. Then the system (1.6) is consistent if and only if.**

$$C_j B_j^{+} B_j = C_j, j = 2,4; QL_N = 0,$$

in which case, the general solution of (1.6) can be expressed as the following:

$$X = C_2 B_2^{+} + QN^{+} R_{B_2} + ZR_N R_{B_2}$$

where Z **is an arbitrary matrix over** H **with compatible dimensions.**

3. THE VARIOUS SYMMETRIC SOLUTIONS TO SOME QUATERNION MATRIX EQUATIONS

In this section, we use Theorem 2.3 to consider the bisymmetric solution to the matrix equation (1.1), the centrosymmetric solution to the system (1.2) and the persymmetric solutions to the systems (1.4). We denote the $n \times n$ **permutation matrix whose elements along the southwest northeast diagonal are ones and whose remaining elements are zeros by** V_n**. By** $[22]$**, we have the following definition.**

Definition 3.1. Suppose that

$$A = (a_{ij}) \in \mathrm{H}^{m\times n}, A^{*} = \left(\overline{a_{ji}}\right) \in \mathrm{H}^{n\times m}, A(*) = \left(\overline{a_{m-j+1,n-i+1}}\right) \in \mathrm{H}^{n\times m},$$

$A^{\#} = \left(a_{m-i+1,n-j+1}\right) \in \mathrm{H}^{m\times n}$**, where** $\overline{a_{ji}}$ **is the conjugate of the quaternion** a_{ji}**,**

then $A^{(*)} = V_n A^* V_m, A^{\#} = V_m A V_n$.

(i) The matrix $A=(a_{ij}) \in \mathrm{H}^{n\times n}$ **is called symmetric if** $A = A^*$.

(ii)The matrix $A=(a_{ij}) \in \mathrm{H}^{n\times n}$ **is called persymmetric if** $A = A^{(*)}$.

(iii)The matrix $A=(a_{ij}) \in \mathrm{H}^{m\times n}$ **is called centrosymmetric if** $a_{ij} = a_{m-i+1,n-j+1}$, i.e. $A = A^{\#}$.

(iv)The matrix $A=(a_{ij}) \in \mathrm{H}^{n\times n}$ **is called bisymmetric if** $a_{ij} = a_{n-i+1,n-j+1} = \overline{a_{ji}}$.

Remarks 3.1. (1) Of the three matrix properties --- symmetric, persymmetric and centrosymmetric --- any two imply the third one. So a bisymmetric matrix A **implies** $A = A^* = A^{(*)} = A^{\#}$

(2) $V_n = V_n{}^{(*)} = V_n{}^{\#} = V_n{}^*$.

(3) For matrices A **and** B **over** H**, it is easy to verify that**

$$(AB)^* = B^* A^*, (AB)^{(*)} = B^{(*)} A^{(*)}, (AB)^{\#} = A^{\#} B^{\#},$$
$$(A^+)^{\#} = (A^{\#})^+, (A^+)^{(*)} = \left(A^{(*)}\right)^+, (A^+)^* = (A^*)^+$$

3.1. The Bisymmetric Solution to (1.3).

Now we use Theorem 2.3 to give a necessary and sufficient condition for the matrix equation (1.3) to have a bisymmetric solution and the expression of such a solution.

Theorem 3.1. Let $B, C \in \mathrm{H}^{n\times m}$ **be known and** $X \in \mathrm{H}^{n\times m}$ **unknown; and**

$$K = B^{(*)} L_{B^*}, N = R_B B^{\#}, M = L_{B^*} L_K, T = C^{(*)} - B^{(*)} (B^*)^+ C^*, Q_1 = T - KCB^+,$$
$$Q = C^{\#} - \left(CB^+\right)^* B^{\#} - L_{B^*} CB^+ B^{\#} - L_{B^*} K^+ TN.$$

Then the matrix equation (1.3) has a bisymmetric solution if and only if

$$KK^+ TR_B = Q_1, QL_N = 0, R_M Q = 0, B^+ BC = C, C^* B = B^* C,$$

in which case, the general bisymmetric solution of (1.3) can be expressed as the following:

$$X = \frac{1}{4}\left(X_1 + X_1{}^* + X_1{}^{(*)} + X_1{}^{\#}\right) \qquad \textbf{(3.1)}$$

with

$$X_1 = (CB^+)^* + L_{B^*} CB^+ + L_{B^*} K^+ TR_B + QN^+ R_B + MZR_N R_B$$

where Z **is an arbitrary matrix over** H **with compatible dimension.**

Proof. It is sufficient to show that the matrix equation (1.3) has a bisymmetric solution is equivalent to the following system

$$\begin{cases} B^{*}X = C^{*} \\ XB = C \\ B^{(*)}X = C^{(*)} \\ XB^{\#} = C^{\#} \end{cases} \tag{3.2}$$

is consistent for X. In fact, if the matrix equation (1.3) has a bisymmetric solution X, then X is obviously a solution of (3.2). Conversely, assume that (3.2) has a solution X_1, then $X^{*}{}_1B = C, X_1{}^{(*)}B = C, X_1{}^{\#}B = C.$ Hence it is easy to verify that (3.1) is a bisymmetric solution of the matrix equation (1.3). Theorem 2.3 yields the remaining part of the proof.

Remark 3.2. (1) Similarly, we can investigate the bisymmetric solution to the quaternion matrix equation (1.1).

(2) Using Theorem 3.1, we can study the bisymmetric solution to the system (1.2), (1.4) and (1.6). In fact, the system (1.2), (1.4) and (1.6) has a bisymmetric solution is equivalent to the following system

$$\begin{bmatrix} A_1 \\ B_2^{*} \end{bmatrix} X = \begin{bmatrix} C_1 \\ C_2^{*} \end{bmatrix}$$

$$\begin{bmatrix} A_1 \\ A_3 \end{bmatrix} X = \begin{bmatrix} C_1 \\ C_3 \end{bmatrix}$$

$$\begin{bmatrix} B_2^{*} \\ B_4^{*} \end{bmatrix} X = \begin{bmatrix} C_2^{*} \\ C_4^{*} \end{bmatrix}$$

has a bisymmetric solution, respectively.

3.2. The Centrosymmetric Solution to the system (1.2).
Now we use Theorem 2.3 to consider the centrosymmetric solution to the system (1.2).

Theorem 3.2.

Let $A_1 \in \mathrm{H}^{m\times n}, B_2 \in \mathrm{H}^{r\times s}, C_1 \in \mathrm{H}^{m\times r}, C_2 \in \mathrm{H}^{n\times s}$ be unknown matrices and $X \in \mathrm{H}^{n\times r}$ unknown; and

$$K = A_1^{\#}L_{A_1}, M = L_{A_1}L_K, N = R_{B_2}B_2^{\#}, T = C_1^{\#} - A_1{}^{\#}A_1 + C_1, Q_1 = T - KC_2B_2^{+},$$

$$Q = C_2^{\#} - A_1^{+}C_1B_2^{\#} - L_{A_1}C_2B_2^{+}B_2^{\#} - L_{A_1}K^{+}TN .$$

Then the system (1.2) has a centrosymmetric solution if and only if

$$KK^{+}TR_{B_2} = Q_1, QL_N = 0, R_M Q = 0,$$
$$A_1A_1^{+}C_1 = C_1, A_1C_2 = C_1B_2, C_2B_2^{+}B_2 = C_2,$$

in which case, the general centrosymmetric solution of (1.2) can be expressed as the following:

$$X = \frac{1}{2}(X_1 + X_1^{\#}) \qquad \textbf{(3.3)}$$

with

$$X_1 = A_1^{+}C_1 + L_{A_1}C_2B_2^{+} + L_{A_1}K^{+}TR_{B_2} + QN^{+}R_{B_2} + MZR_NR_{B_2}$$

where Z is an arbitrary matrix over H with compatible dimensions.

Proof. It is sufficient to show that the system (1.2) has a centrosymmetric solution equivalent to the system

$$\begin{cases} A_1X = C_1 \\ XB_2 = C_2 \\ A_1^{\#}X = C_1^{\#} \\ XB_2^{\#} = C_2^{\#} \end{cases} \qquad \textbf{(3.4)}$$

is consistent for X. As a mater of fact, if the system (1.2) has a centrosymmetric solution X, then X is obviously a solution of the system (3.4). Conversely, suppose that the system (3.4) has a solution X_1. Noting that $A_1X_1^{\#} = C_1, X_1^{\#}B_2 = C_2$ by $A_1^{\#}X_1 = C_1^{\#}$ and $X_1B_2^{\#} = C_2^{\#}$. Hence it is easy to verify that (3.3) is a centrosymmetric solution of the system (1.2). The remaining parts of the proof can be obtained by Theorem 2.3.

3.3. The Persymmetric Solution to (1.4).
Now we consider the persymmetric solution to the system (1.4) by using Theorem 2.3.

Theorem 3.3.
Let $A_1, C_1 \in \mathrm{H}^{m\times n}, A_3, C_3 \in \mathrm{H}^{k\times n}$ be known matrices and

$$K = A_3L_{A_1}, M = L_{A_1}L_K, N = R_{A_1^{(*)}}A_3^{(*)}, T = C_3 - A_3A_1^{+}C_1, Q_1 = T - K(A_1^{+}C_1)^{(*)},$$
$$Q = C_3^{(*)} - A_1^{+}C_1A_3^{(*)} - L_{A_1}(A_3A_1^{+}C_1)^{(*)} - L_{A_1}K^{+}TN .$$

Then the system (1.4) has a persymmetric solution if and only if

$$A_i A_i^{+} C_i = C_i, i = 1,3, KK^{+} TR_{A_1^{(*)}} = Q_1, QL_N = 0, R_M Q = 0,$$

in which case, the general solution of (1.4) can be expressed as the following:

$$X = \frac{1}{2}\left(X_1 + X_1^{(*)}\right) \tag{3.5}$$

with

$$X_1 = A_1^{+} C_1 + L_{A_1}(A_1^{+} C_1)^{(*)} + L_{A_1} K^{+} TR_{A_1^{(*)}} + QN^{+} R_{A_1^{(*)}} + MZR_N R_{A_1^{(*)}}$$ **w**

here Z **is an arbitrary matrix over** H **with compatible dimensions.**

Proof. It is sufficient to show that the system (1.4) has a persymmetric solution is equivalent to the system

$$\begin{cases} A_1 X = C_1 \\ XA_1^{(*)} = C_1^{(*)} \\ A_3 X = C_3 \\ XA_3^{(*)} = C_3^{(*)} \end{cases} \tag{3.6}$$

is consistent for X **. In fact, if the system (1.4) has a persymmetric solution** X **, then** X **is obviously a solution of the system (3.6). Conversely, assume that the system (3.6) has a solution** X_1**. Noting that** $A_1 X_1^{(*)} = C_1, A_3 X_1^{(*)} = C_3$ **by** $XA_1^{(*)} = C_1^{(*)}$ **and** $XA_3^{(*)} = C_3^{(*)}$**. Hence it is easy to verify that (3.5) is a persymmetric solution of the system (1.4). The remaining parts of the proof can be obtained by Theorem 2.3.**

Remark 3.3. Similarly we can investigate the persymmetric solution of the system (1.6).

REFERENCES

1. **C.G. Khatri and S.K. Mitra, Hermitian and nonnegative definite solutions of linear matrix equations, SIAM J. Appl. Math. 31 (1976): 578-585.**
2. **L. Wu, B. Cain, The Re-nonnegative define solutions to the matrix inverse problem AX=B, Linear Algebra Appl. 236 (1996): 137-146**
3. **L. Wu, The Re-positive define solutions to the matrix inverse problem AX=B, Linear Algebra Appl. 174(1992): 145-1151.**
4. **J. Groβ, Expicit solutions to the matrix inverse problem AX=B, Linear Algebra Appl. 289 (1999): 131-134.**
5. **W.J. Vetter, Vector structures and solutions of linear matrix equations, Linear Algebra Appl. 9 (1975):181-188.**
6. **J.R. Magnus and H. Neudecker, The elimination matrix: Some**

lemmas and applications, SIAM J. Algebraic Discrete Methods 1(1980): 422-428.

7. K.E. Chu, symmetric solutions of linear matrix equations by matrix decomposition, Linear Algebra Appl. 119(1989):35-50.
8. F.J. Henk Don, On the symmetric solutions of a linear matrix equation, Linear Algebra Appl. 93 (1987):1-7.
9. H. Dai, On the symmetric solution of linear matrix equations, Linear Algebra Appl. 131 (1990) 1-7.
10. S.K. Mitra, The matrix equations $AX = C, XB = D,$ Linear Algebra Appl. 59 (1984):171-181.
11. A.C. Aitken, Determinants and Matrices, Oliver and Boyd, Edinburgh, 1939.
12. L. Datta and S.D. Morgera, On the reducibility of centrosymmetric matrices-applications in engineering problems, Circuits system sig. Proc. 8(1) (1989): 71-96.
13. A. Cantoni and P. Butler, Eigenvalues and eigenvectors of symmetric centrosymmetric matrices, Linear Algebra Appl. 13 (1976): 275-288.
14. J.R. Weaver, Centrosymmetric (cross-symmetrisc) matrices, their basic properties, eigenvalues, eigenvectors, Amer. Math Monthly 92 (1985): 711-717.
15. A. Lee, Centrohermitian and skew-centrohermitian matrices, Linear Algebra Appl. 29 (1980): 205-210.
16. R.D. Hell, R.G. Bates and S.R. Waters, On centrohermitian Matrices, SIAM J. Matrix Anal. Appl. 11(1) (1990): 128-133.
17. R.D. Hell, R.G. Bates and S.R. Waters, On perhermitian matrices, SIAM J. Matrix Anal. Appl. 11(2) (1990): 173-179.
18. Russell M. Reid, Some eigenvalues properties of persymmetric matrices, SIAM Rev. 39 (1997): 313-316.
19 A.L. Andrew, Centrosymmetric matrices, SIAM Rev. 40 (1998): 697-698.
20. I.S. Pressman, Matrices with multiple symmetry properties: applications of centrohermitian and perhermitian matrices, Linear Algebra Appl. 284(1998): 239-258
21. A. Melman, Symmetric centrosymmetric matrix – vector multiplication, Linear Algebra Appl. 320 (2000): 193-198.
22. Q.W. Wang, J.H. Sun, S.Z. Li, Consistency for bi(skew) symmetric solutions to systems of generalized Sylvester equations over a finite central algebra, Linear Algebra Appl. 353 (2002): 169-182.
23. Q.W. Wang, A system of matrix equations and a linear matrix equation over arbitrary regular rings with identity, Linear Algebra Appl. 384 (2004): 43-54.

PK ISSN 0022- 2941; CODEN JNSMAC
Vol. 46, No.1 & 2 (April & October 2006) PP 13-19

SOME RESULTS ON DERIVATIONS OF BCI-ALGEBRAS

Hamza A. S. Abujabal, and Nora O. Al-Shehri
Mathematics Department, Faculty of Sciences, King Abdulaziz University, P. Box 80009, Jeddah 21589, Saudi Arabia.

(Received: July 7, 2006)

ABSTRACT: In this note, we investigate some fundamental properties and prove some results on derivations of BCI-algebras.

1. INTRODUCTION

In the theory of rings and near rings, the properties of derivations is an important topic to study [8, 10]. In [7], Jun and Xin applied the notions of rings and near rings theory to BCI- algebras and obtained some properties. In this paper, we prove some results on derivations of BCI-algebras. First, we show that a derivations of BCK-algebra is regular and prove that if d is a derivation of a BCI-algebra X and $\alpha \in X$ such that $a * d(x) = 0$ or $d(x) * a = 0$, for all $x \in X$, then d is regular and X is a BCK-algebra. Also we study a derivation of a $p-$semisimple BCI-algebra X, then d_1, d_2 are derivations of a $p-$semisimple BCI-algebra X, then $d_1 \circ d_2$ is also a derivation of X and $d_1 \circ d_2 = d_2 \circ d_1$. Finally, we show that $d_1 * d_2 = d_2 * d_1$, where d_1, d_2 are derivations of a $p-$semisimple BCI-algebra X.

2. PRELIMINARIES

Let X be a set with a binary operation * and a constant 0. Then $(X, *, 0)$ is called a BCI-algebra, if it satisfies the following axioms for all $x, y, z \in X$:

BCI-1: $((x * y) * (x * z)) * (z * y) = 0$;
BCI-2: $(x * (x * y)) * y = 0$;
BCI-3: $x * x = 0$;
BCI-4: $x * y = 0$ **and** $y * x = 0$ **imply** $x = y$ **[6].**

Define a binary relation $\leq$ on X by putting $x \leq y$ if and only if $x * y = 0$. Then $(X; \leq)$ is a partially ordered set. A BCI-algebra X satisfying $0 \leq x$, for all $x \in X$, is called a BCK-algebra. In any BCI-algebra X, the following hold [6] for all $x, y, z \in X$:

(1) $x * 0 = x$.
(2) $(x * y) * z = (x * z) * y$.
(3) $0 * (x * y) = (0 * x) * (0 * y)$.
(4) $* (x * (x * y)) = x * y$ **[1].**
(5) $((x * z) * (y * z)) * (x * y) = 0$.
(6) $x \leq y$ **implies** $x * z \leq y * z$ **and** $z * y \leq z * x$.
(7) $x * 0 = 0$ **implies** $x = 0$.

For a BCI-algebra X**, denote by** $X_+ = \{x \in X \mid 0 \leq X\}$**, the BCK-part of** X**, and by** $G(X) = \{x \in X \mid 0 * x = x\}$**, the BCI-G part of** X**. If** $X_+ = \{0\}$**, then** X **is called a** $p-$**semisimple BCI – algebra. For all** $x, y, z \in X$**, the following hold in a *p*-semisimple BCI-algebra** X**:**

(8) $(x * z) * (y * z) = x * y$.
(9) $0 * (0 * x) = x$.
(10) $x * (0 * y) = y * (0 * x)$.
(11) $x * y = 0$ **implies** $x = y$.
(12) $x * y = x * z$ **implies** $y = z$.
(13) $y * x = z * x$ **implies** $y = z$.
(14) $y * (y * x) = x$ **[3, 4, 5, 11]**

Let X be a BCI-algebra. We denote $x \wedge y = y * (y * x)$**, For more details, we refer to [2, 9, 12, 13].**

Definition 2.1 [7] Let X be a BCI-algebra. By a (ℓ, r**) – deviation of X, we mean a self map** d **of** X **satisfying the identity** $d(x * y) = d(x) * y \wedge x * d(y)$, **for all** $x, y \in X$**. If X satisfies the identity** $d(x * y) = x * d(y) \wedge d(x) * y$, **for all** $x, y \in X$, **then we say that d is a** (r, ℓ)**- derivation of** X**. Moreover, if** d **is both a** (ℓ, r) **and a** (r, ℓ)**-derivation, we say that** d **is a derivation of X.**

Definition 2.2 [7]. A self map d **of BCI-algebra X is said to be regular if** $d(0) = 0$.

Proposition 2.3 [7] Let d **be a regular derivation of BCI-algebra** X**. Then the following hold:**

(i) $d(x) \le x$ *for all* $x \in X$.

(ii) $d(x) * y \le x * d(y)$, *for all* $x, y \in X$.

(iii) $d(x * y) = d(x) * y \le d(x) * d(y)$, *for all* $x, y \in X$.

(iv) $d^{-1}(0) = \{x \in X \mid d(x) = 0\}$ *is a subalgebra of* X *and* $d^{-1}(0) \subset X_+$.

3. SOME RESULTS ON DERIVATIONS

First, we study derivations on BCK-algebras:

Proposition 3.1: Every (r, ℓ)-derivations (or a (ℓ, r)-derivation) of a BCK-algebra is regular.

Proof. Let X is a BCK-algebra and d a (r, ℓ)-deviation of a X. Then for all $x \in X$, we have:

$$d(0) = d(0 * x) = 0 * d(x) \wedge d(0) * x$$
$$= 0 \wedge d(0) * x = 0$$

Now let d is a (ℓ, r)-deviation of X. Then for all $x \in X$ we have:

$$d(0) = d(0 * x) = d(0) * x \wedge 0 * d(x)$$
$$= d(0) * x \wedge 0 = 0$$

From Proposition 3.1 we get:

Corollary 3.2: A derivation of a BCK-algebra is regular.

In Proposition 3.3 (resp. Proposition 3.4), we assume that d is a derivation of a BCI-algebra X and $a \in X$ such that $d(x) * a = 0$, (resp. $a * d(x) = 0$), for all $x \in X$, then we show that d is a regular derivation of X and X is a BCK-algebra:

Proposition 3.3. Let d be a derivation of a BCI-algebra X and $a \in X$ such that $d(x) * a = 0$, for all $x \in X$. Then d is a regular derivation of X. Moreover X is a BCK-algebra.

Proof. Let d be a derivation of a BCI-algebra X and let $a \in X$ such that $d(x) * a = 0$, for all $x \in X$. Since d is (ℓ, r)-derivation we get:

$$0 = d(x * a) * a = (d(x) * a \wedge x * d(a)) * a$$
$$= 0 \wedge x * d(a)) * a = 0 * a$$

thus $0 \le a$, and so $x \in X_+$. This shows that

$$d(0) = d(0 * a) = d(0) * a \wedge 0 * d(a)$$
$$= 0 \wedge 0 * d(a) = 0$$

Hence d **is a regular derivations of** X **. So by Proposition 2.3 (i) we have** $d(x) \le x,$ **for all** $x \in X$ **and so.**

$$0 * x \le 0 * d(x) = (d(x) * a) * d(x)$$
$$= 0 * a = 0$$

Thus $0 * x \le 0$ **for all** $x \in X$ **and so** $0 = (0 * x) * 0 = 0 * x$ **. Then we have** $0 \le x$ **, for all** $x \in X$ **. Which implies that** X **is a BCK-algebra.**

Similarly we can prove:

Proposition 3.4. Let d **be a derivation of a BCI-algebra** X **and** $a \in X$ **such that** $a * d(x) = 0,$ **for all** $x \in X$**. Then** d **is a regular derivation of** X **. Moreover,** X **is a BCK-algebra.**

Finally, we study a derivations of a $p-$ **semisimple BCI-algebra:**

Definition 3.5: Let X **be a BCI-algebra and** d_1, d_2 **two self maps of** X **We define d1. d2** $d_1 \circ d_2 : X \to X$ *as*:

$$d_1 \circ d_2(x) = d_1(d_2(x)), \text{ for all } x \in X.$$

Proposition 3.6 Let X **be a** $p-$ **semisimple BCI-algebra and** d_1 **,** d_2 **the** (ℓ, r) **-derivations of** X **. Then** $d_1 \circ d_2$ **is also a** (ℓ, r) **-derivation of** X **.**

Proof. Let X **be a** $p-$ **semisimple BCI – algebra and** d_1, d_2 **are** (ℓ, r) **-derivations of** X **. Then by (14) and proposition 2.3 (ii), we get for all** $x, y \in X$ **:**

$$(d_1 \circ d_2)(x * y) = d_1(d_2(x) * y \wedge x * d_2(y)) = d_1(d_2(x) * y)$$
$$= d_1(d_2(x)) * y \wedge d_2(x) * d_1(y) = d_1(d_2(x)) * y$$
$$= (x * d_1(d_2(y))) * ((x * d_1(d_2(y))) * (d_1(d_2(x)) * y))$$
$$= (d_1 \circ d_2)(x) * y \wedge x * (d_1 \circ d_2)(y)$$

Which implies that $d_1 \circ d_2$ **is a** (ℓ, r) **- derivation of** X .

Similarly, we can prove:

Proposition 3.7. Let X **be a** $p-$ **semisimple BCI –algebra and** d_1, d_2 **are** (r, ℓ) **–derivations of** X **. Then d1 d2 is also a** (r, ℓ) **–derivation of** X **.**

Combining Propositions 3.6 and 3.7, we get:

Theorem 3.8. Let X **be a** $p-$**semisimple BCI –algebra and** d_1, d_2 **derivations of X. Then** $d_1 \circ d_2$ **is also a derivation of X.**

Proposition 3.9. Let X **be a** $p-$**semisimple BCI –algebra and** d_1, d_2 **derivations of X. Then** $d_1 \circ d_2 = d_2 \circ d_1$**.**

Proof. Let X **be a** $p-$**semisimple BCI –algebra and** d_1, d_2**, the derivations of X. Since** d_2 **is a** (l,r)**–derivation of** X**, then for al** $x, y \in X$**:**

$$d_1 \circ d_2(x * y) = d_1\big(d_2(x * y)\big) = d_1\big(d_2(x) * y \wedge x * d_2(y)\big)$$
$$= d_1\big(d_2(x) * y\big)$$

But d_1 **is a** (r,l)**-derivation of** X**, so**

$$(d_1 \circ d_2)(x * y) = d_1\big(d_2(x) * y\big)$$
$$= d_2(x) * d_1(y) \wedge d_1\big(d_2(x)\big) * y$$
$$= d_2(x) * d_1(y)$$

thus we have for all $x, y \in X$**:**

$$(d_1 \circ d_2)(x * y) = d_2(x) * d_1(y) \qquad \textbf{(1)}$$

Also, since d_1 **is a** (r,l)**-derivation of** X**, then for all** $x, y \in X$**:**

$$\big(d_2 \circ d_1\big)(x * y) = d_2\big(x * d_1(y) \wedge d_1(x) * y\big)$$
$$= d_2\big(x * d_1(y)\big)$$

But d_2 **is a** (l,r)**-derivation of X, so**

$$\big(d_2 \circ d_1\big)(x * y) = d_2\big(x * d_1(y)\big)$$
$$= d_2(x) * d_1(y) \wedge x * d_2\big(d_1(y)\big)$$
$$= d_2(x) * d_1(y)$$

Thus we have for all $x, y \in X$**:**

$$\big(d_2 \circ d_1\big)(x * y) = d_2(x) * d_1(y) \qquad \textbf{(2)}$$

From (1) and (2) we get for all $x, y \in X$**:**

$$\big(d_1 \circ d_2\big)(x * y) = \big(d_2 \circ d_1\big)(x * y)$$

By putting $y = 0$ **we get for all** $x \in X$ **:**

$$(d_1 \circ d_2)(x) = (d_2 \circ d_1)(x)$$

Which implies that $d_1 \circ d_2 = d_2 \circ d_1$

Definition 3.10. Let X **be a BCI-algebra and** d_1, d_2**, two self maps of** X **. We define** $d_1 * d_2 : X \longrightarrow X$ *as* **:**

$(d_1 * d_2)(x) = d_1(x) * d_2(x)$, **for all** $x \in X$

Proposition 3.11. Let X **be a** $p-$**semisimple BCI –algebra and** d_1, d_2 **derivations of** X **. Then** $d_1 * d_2 = d_2 * d_1$

Proof. Let X **is a** $p-$**semisimple BCI –algebra and** d_1, d_2 **derivations of** X **. Since** d_2 **is a** (l,r)**-derivation of** X **, then for all** $x, y \in X$ **:**

$$(d_1 \circ d_2)(x * y) = d_1(d_2(x) * y \wedge x * d_2(y)) = d_1(d_2(x) * y)$$

But d_1 **is a** (r,l)**-derivation of** X **, so**

$$\begin{aligned} d_1(d_2(x) * y) &= d_2(x) * d_1(y) \wedge d_1(d_2(x)) * y \\ &= d_2(x) * d_1(y) \end{aligned}$$

hence

$$(d_1 \circ d_2)(x * y) = d_2(x) * d_1(y) \text{ for all } x, y \in X \qquad (3)$$

Also, we have that d_2 **is al** (r,l) **-derivation of** X **, then for all** $x, y \in X$ **:**

$$(d_1 \circ d_2)(x * y) = d_1(x * d_2(y) \wedge d_2(x) * y) = d_1(x * d_2(y))$$

But d_1 **is a** (l,r) **- derivation of** X **, so**

$$\begin{aligned} d_1(x * d_2(y)) &= d_1(x) * d_2(y) \wedge x * d_1(d_2(y)) \\ &= d_1(x) * d_2(y) \end{aligned}$$

Thus

$$(d_1 \circ d_2)(x * y) = d_2(x) * d_2(y) \text{ for all } x, y \in X \qquad (4)$$

From (3) and (4) we get:

$$d_2(x) * d_1(y) = d_1(x) * d_2(y) \quad \text{for all } x, y \in X$$

By putting $x = y$ **we get for all** $x \in X$ **:**

$$d_2(x) * d_1(x) = d_1(x) * d_2(x)$$
$$(d_2 * d_1)(x) = (d_1 * d_2)(x)$$

Which implies that $d_2 * d_1 = d_1 * d_2$

4. REFERENCES

1. **B. Ahmad, On Iseki's Bci-algebras, Jr.of Natural Sciences and Mathematics, 8(1980), 125-130.**
2. **M. Aslam and A.B. Thaheem, A note on p-semisimple BCI-algebras, Math. Japon., 36 (1), (1991) , 39-45.**
3. **M. Daoji, BCI-algebras and Abelian Groups, Math. Japonica, 35 (5), (1987), 693-696**
4. **W.A. Dudeck, On BCI-algebras with condition(s), Math. Japonica, 31(1), (1986), 26-29**
5. **C.S. Hoo, BCI-algebras with condition (s), Math. Japonica, 32 (5), (1987), 749-756.**
6. **K. Iseki, On BCI-algebras, Math. Sem. Notes, 8(1980), 125-130**
7. **Y.B. Jun and X.L. Xin, On derivations of BCI-algebras, Inform. Sci., 159 (2004), 167-176.**
8. **P. H. Lee and T.K. Lee, On derivations of Prime rings, Chinese J. Math. 9 (1981), 107-110**
9. **J. Meng, Y.B. Jun and E.H. Roh, BCI-algebras of order 6, Math. Japon. 47 (1) (1998), 33-43**
10. **E. Posner, Derivations in prime rings, Proc. Amer. Math. Soc., 8 (1957), 1093-1100.**
11. **L.Tiande and X.Changchang, p-Radical in BCI-algebras, Math. Japonica, 30 (4), (1985), 511-517.**
12. **X.L. Xin, E.H. Roh and J.C.Li, Some results on the BCI-G part of algebras, Far East J. Math Sci. Special Volume (Part III), (1997), 363-370.**
13. **Q. Zhang, Some other characterizations of p-semisimple BCI – algebras, Math. Japon., 36 (5) (1991), 815-817.**

PK ISSN 0022- 2941; CODEN JNSMAC
Vol. 46, No.1 & 2 (April & October 2006) PP 21-32

STUDIES ON THREE EXCESS PROPERTIES OF BINARY LIQUID MIXTURES OF 1-BUTYLAMINE WITH SOME ALCOHOLS AT TWO DIFFERENT TEMPERATURES

S. Shakeel Ahmad*, Mohammad Yaqub and Abid Karim
Materials Science Research Centre,
PCSIR Laboratories Complex, Karachi-75280

(Received: October 14, 2006)

Abstract: A thermodynamic study of liquid mixtures was under taken, which is based on Grunberg's law of mixture viscosity and change in the activation energy of viscous flow. The excess partial molar volume V^E of three different 1-butylamine+alcohol mixtures, that belongs to excess function with the strongest negative values were studied. The viscosity deviation $\Delta\eta$, excess viscosity η^E, and the excess Gibb's energy of activation, ΔG^{*E} of the viscous flow were calculated from the density and viscosity data of three binary mixtures via 1-butylamine+ethanol, 1-butylamine+1-propanol and 1-butylamine+heptanol at temperatures of 303.15K and 313.15 K. The viscosity data have been correlated with Grumberg-Nissan equation*, which is equal to the sum of the products of each mole fraction x_1 with individual viscosity. A generalized version is presented which allows the description of excess properties, via density, Gibb's energy and viscosity of three binary mixtures with two associated components, provided one of these component shows a weak self association. As a result of this strong intermolecular association, the three systems were found to have a very large excess molar volume. With increase in concentration of alcohol in amines, the excess molar volume is high initially, but decreases gradually before attaining its original value. The magnitude of negative deviation increases with chain length of alcohol.

KEY WORDS: Binary Liquid mixture , Excess molar volume, Thermodynamic, Gibb's Energy of Activation, Density, viscosity and molar interaction.

1. INTRODUCTION

The Visco-elastic properties of a mixture of two organic compounds depends on their ratio of components during mixing states. If the two components are completely compatible with each other, the mixed system behaves like a random copolymer with only one glass transition temperature, which is a function of their molecular ratio [2-4]. There may exist a strong interaction between their molecules. It has been suggested that these intermolecular forces are resulting from the polymerization of molecules induced by their atoms. It is well known that alcohol as well as amine molecules have a pronounced tendency to form associated species due to hydrogen bonding effect [1,2]. A consistent molecular model can be formed which accounts for self association of alcohol in pure state and in alcohol-amine mixtures [14,15]. Amine or its derivatives butyl amine are

being increasingly used in making many commercial and industrial products made through chemical reaction and processes.

The amines are the derivatives of ammonia NH_3, where one, two or all three hydrogen atoms are replaced by univalent hydrocarbon radicals. Depending upon the number of hydrogen atoms in NH_3 so replaced, primary, secondary and tertiary amines are obtained. In chemical industry this has stimulated the need for extensive information on thermodynamic and transport properties of such types of mixtures [9-12]. For schematic investigation of thermodynamic properties, acoustical behavior and transport properties, their viscosities,densities and ultrasonic velocity with compressibility at various temperatures have to be considered [5-8]. The chemical behavior of all amines is greatly influenced by whether it is primary, secondary and tertiary. The secondary and tertiary amines are soluble in alcohols but have a very limited water solubility. The excess molar volume is one of the basic thermodynamic quantity of liquid mixtures and enormous amount of data on such long chain compounds have been collected in the literature [8-10]. In the present study, an attempt was made to describe schematically the properties of liquid mixtures, based on current solution theory and the cell model theory and the regular solution theory [9-11]. Although these theories have helped in explaining the excess thermodynamic functions of non polar binary mixtures, so far only quantitative agreement has been obtained for polar binary mixtures [13-15]. An attempt has been made to describe quantitatively the properties of liquid mixtures which are based on current solution theories, the cell model theory. Funke. H. *et al* [11] presented an extended and real associated solution model for the thermodynamic functions that is Excess Gibbs energy of activation for alcohol +amine mixture which was originally developed for describing the alcohol +hydrocarbon mixing properties.

Both the primary amines and the above three alcohols are proton donor and proton acceptor. It is expected that there will be a significant degree of H-bonding, in (H---H), leading to self association in pure state, in addition to mutual association between their binary species A and B. Besides AB and Ai B mixed associates, the species A_i B_j also exists .The latter species contains many monomers and can be formed with or without breaking of H-bond present in the pure liquid. The purpose of such studies is to throw some light on the formation of mixed species as well as their influence on the excess properties of the mixtures. An additional objective was to study the presence of excess molar volume due to several expansion and contraction processes which proceed simultaneously during reaction, when amine+ alcohol mixtures are formed [16-18].The work is expected to provide a test of various empirical equations to correlate the Grumberg Nissan equations* [19] for viscosity law with the data of binary mixtures containing both the polar components.

2. CALCULATIONS

MIXTURE LAW OF VISCOSITY:

Grumberg and Nissan* in 1949, presented an expression for the viscosity of a solution which consists of more than one components of different mole fraction N_1 to N_2 and viscosity η_1 and η_2 of component 1 and 2 , similarly for component 3. However both the +ve and –ve deviations from the above equations are found to occur. From a comparison of vapor pressure and viscosity data of the solutions, the following equations* have been deduced [19].

$$\text{Log } \eta_{s+} = N_1 \log\eta_1 + N_2 \log\eta_2 + N_3 \log\eta_3 \quad \text{(1)}$$

Where η_{s+} is the viscosity of the overall solution.

Excess molar volume V^E was calculated from the molar mass Mi, given by equation (2) and the densities of pure liquid and its mixture as [6]

$$V^E = \Sigma x_i M_i (1/\rho - 1/\rho_i) \text{ cm}^3/\text{mole} \quad \text{(2)}$$

Where ρ is the density of pure liquid and ρ_i density of mixture containing ith component. After mixing the relative change in volume Δv, Reiman has suggested an equation (3) [4].

$$\Delta v = V^E / \Sigma_{i=1}^{2} x_i v_i \quad \text{(3)}$$

where x_i is the mole fraction , v_i is the volume of ith component.

The change in viscosity $\Delta\eta$, from a linear dependence on mole fraction were calculated by equation (4)[17,18].

$$\Delta\eta = \eta - \Sigma x_i \eta_i \quad \text{(4)}$$

The deviations of the viscosity $\Delta\eta$, from the ideal mixture values i.e excess viscosity η^E were calculated as per absolute rate reaction theory is given by Glasstone and Erying [5,6]

$$\eta^E = \eta - \exp [\Sigma x_i \log \eta_i] \quad \text{(5)}$$

η_l is the viscosity of pure component. On the basis of theory of absolute rate reaction , the excess Gibb's energy of activation , $\underline{\Delta G^{\#E}}$ in J /mole, of viscous flow is calculated from equation (6) ,

$$\frac{\Delta G^{\#E}}{RT} = [\ln(\eta V/\eta_2 V_2) - X_1 \ln (\eta_1 V_1/\eta_2 V_2)] \quad \text{(6)}$$

Where V is the molar volume of the mixture, η_1, η_2, are the viscosity of component 1 and 2, V_1 is the molar volume of pure component 1, V_2 is the molar volume for component 2 and V^E and ΔG^{*E} are the excess molar volume and excess Gibb's energy of activation respectively. The estimated

accuracy of excess molar volume is 0.005 ml/mole and $\Delta G^{\#\,E}$ is about 20 J /mole. These equations from 1 to 6 called the correlating equations.

EXPERIMENTAL

Sample preparation : The samples were prepared by mixing a known mass of pure liquids in an air tight flask (volumetric) so that to have minimum loss from evaporation. The weight is measured by OHAUS Physical balance, which is an electronic type and based on load cell. It is accurate down to $\pm$0.01mg. The possible error in the mole fraction is estimated to be less than $\pm$ 2.5x10^{-4} gm/ml. The viscosity were reproducible to within $\pm$ 5x10^{-3}millipoise, the densities were reproducible to within $\pm$2x10^{-3}gm/ml

CHEMICAL REAGENTS AND PURITY OF THE SAMPLES:

All the liquids including 1- butyl amine were of A.R grade obtained from Merck- Schuchardt. German ,used after the process of purification.. Through HPLC process of purification .and boiling point measurements , the Ethanol , 1-Propanol and heptanol were used after drying over molecular sieve of size 4A. The 1- butyl amine was stored over NaOH pellets for several days and than fractionally distilled. The estimated purity was 99.55% for alcohol and 99.9% for butyl amines. The measured values of density ρ, viscosity η are in good agreement with the literature values [18].

VISCOSITY MEASUREMENTS

Heppler's Falling ball Viscometer has been utilized here for the precise measurement of viscosity of 1-butylamine (pure) and its different mixtures formed with alcohols [ethanol and 1-propanol and heptanol] having viscosity in the range which is greater than 1000 milli poise. The falling ball method is the most convenient for industrial purpose. This method employs a cylinder of liquid through which the rate of falling of steel ball can be observed. The assembly is maintained at constant temperature. In this viscometer the difference between cylinder diameter and the ball diameter is much less. The cylinder is of uniform diameter throughout its e length and is inclined away from the vertical position, permitting ball to roll down ,with the line of contact in the cylinder. The rolling down time of the steel ball was recorded. This instrument can measure a wide range of viscosity. The following equation (7) is used as formula for measuring viscosity η,

$$\eta = KT\,(ds\text{-}dl)\,dt \text{ ---------- (7)}$$

where K is a constant, called ball constant, T is the absolute temperature ,.ds is the distance covered by falling ball, and dl is the length of the liquid column, dt = change in time.

Equipment for density measurements: Calibrated Ostwald- Spregel type pycnometer made of Pyrex Glass with volume 25ml and with 0.1cm dia of

the capiliary tube was used to determine the density of pure solvent and the mixtures. The density ρ of the prepared sample were measured in gm/ml at two temperatures 303.15 K and 313.15 K and duplicate density values agreed to within $\pm 1 \times 10^{-4}$ gm/ml. The samples were kept with thermostatic bath controlled to a temperature of $\pm$ 0.5K.

3. RESULTS AND DISCUSSIONS

The following results have been achieved from this thermodynamic studies of these mixtures within certain experimental error. Fig: 1 and 4 revealed , the values of $(\delta\eta/\delta c)$ called the change in viscosity with concentration which is obvious from the curves at two temperatures 303.15K and 313.15K, the viscosity decreases with the increase in mole fraction of x_1 of butylamine in alcohol for all three binary mixtures approaches to 0.9 m poise. The excess molar volume V^E (Fig 2 & 5) was large and strongly negative at midrange of concentration, for all three butylamine+ alcohol mixtures at both temperatures and over entire range of compositions. The magnitude of negative deviation in excess molar volume decreases with the increase in chain length of alcohol and with the rise in temperature from 303.15K to 313.15K, which is in good agreement with the observation of other workers [20,21].Their values can be expected to reveal some interesting facts concerning the nature of different kinds of hydrogen bonding association constant K, which is less than one and is observed in alcohol+amine mixture. In comparison with amine they are smaller than two orders of magnitude than those found for alcohols 100<K>100. The excess molar volume was calculated from molar mass M_1 and the density of pure liquid ρ the density of mixtures as given ρ_1 in equation (2) and their relative change in volume Δv, as given by equation (3) is also a relevant quantity. As a result of disruption of self association of alcohol and amine by the addition of inert globular hydrocarbon molecules, the large positive deviation of V^E was observed in the case of ROH+C_6H_6 and the butyl amine - C_6H_6 mixtures This suggests positive contribution to the excess molar volume. With the increase in concentration of alcohol in amine, the excess molar volume was decreased first and than increased. The extrapolated values of excess molar volume agree well with those obtained in the earlier studies [11, 12, 13].

The results of the present work indicate not only that the NH group is a weaker proton donor compared to the OH group but also that is a hindrance which play a role in formatting the hydrogen bond in the amine self association, because more groups are involved than in the case of OH-O bonding [9].The density and viscosity of all the mixtures decreases at a particular temperature,fig:1&4 as shown by several other workers too [14,15]. Since our results are at two different temperatures 303.15K and 313.15K, it is not possible to make direct comparison of the viscosity data from the literature. The values of excess molar volume V^E at a temperature 313.15K for butyl amine +heptanol are within some % of tolerance, which is in accordance with the results of Reiman Heintz and others [4,16,19]. The values of Gibb's Energy of activation ΔG^{*E} for equvi

molar mixtures were positive, as shown in Figure# 3 for all three mixtures and decreases from heptanol to ethanol+1-butylamine mixtures. These declined to a minimum value before increasing consistently and attains a minimum value, then increases regularly. Small negative values of ΔG^{*E}. for butylamine + ethanol were observed when mixture has higher concentration of amine , like 0.9mole fraction. ΔG^{*E} decreases with increase in concentration. of alcohol. The present results of excess molar volume can be interpreted qualitatively by taking in to account the fact that several expansion and contraction processes proceed simultaneously when butylamine+ alcohol mixtures are formed. This strong interaction which exceeds the OH-O interaction can be interpreted qualitatively by thinking that free electrons pair located at the N atom has a higher polarizability and therefore acts as a more efficient proton acceptor for OH group than OH itself . The quantum mechanical study of H-bonding in H_2O/NH_3 system was confirms by Allen [9] in the favor of the present results.

EFFECT OF TEMPERATURE ON THE PROPERTIES OF BUTYLAMINE +ALCOHOL MIXTURES.

To account for the temperature effects on excess molar volume, V^E and viscosity η the following points are important. It is known that pure alcohol can form either ring or chain like complexes and while the fraction of ring complexes increases with number of CH_2 group in the alcohol. The degree of association of amine also decreases with rising temperature. The two mixtures of 1- propanol and heptanol with butylamine showing negative deviation from the mole fraction of linearity, except very small positive deviations in the low mole fractions region of butylamine+ ethanol system. The magnitude of negative deviations increased with the chain length of alcohol. As temperature rises the magnitude of negative deviation decreases. The negative values of excess molar volume indicates that the second contribution is more important in determining the sign of excess molar volume. As can be seen from the graph # 5 , the excess viscosity η^E was positive and practically it increases with chain length of alcohols, since the viscosity of higher chain alcohol itself has a high value. Our results show that the values of excess molar volume increases with the increase in temperature when amine alcohol mixtures are formed, several expansion and contraction process proceed simultaneously.

With rising temperature the associated ring breakdown to chain which is then followed by a total breakdown of the associated species. The formation of mixed complex is an exothermic process, hence the equilibrium constant decreases with increasing temperature. The associated ring breakdown to chain with increasing temperatures,which is then followed by a total breakdown of the associated species. The degree of association of amine also decreases with the rising temperature. The formation of mixed complex is an exothermic process, hence the equilibrium constant decreases with the increasing temperature. The two mixtures of 1-`propanol and heptanol showed some negative deviation

from the mole fraction of linearity except very small positive deviations in low mole fraction region of 1- butylamine + ethanol system. The magnitude of negative deviations increases with chain length of alcohol. As the temperature rises the magnitude of negative deviations decreased. The negative values in excess molar volume indicated that the second contribution is more important in determining the sign of excess molar volume [21]. As can be seen from the graph # 4, the excess viscosity η^E are positive and practically it shifts to higher value with chain length of alcohol at very low concentration, since the viscosity of higher chain alcohol itself has a high value. Our results (Fig 5) show that the values of excess molar volume increased with temperature, when amine +alcohol mixtures are formed, here several expansion and contraction process proceeds simultaneously. The strong interaction which exceeds the OH-H interaction can be interpreted qualitatively by thinking that free electron pair located at the N atom which has a higher polarizability and acts as a more efficient proton acceptor for OH group than OH itself. Quantum mechanical study of H-bonding in H_2O/NH_3 system confirms the results thus obtained. Expansion due to de -polymerization of alcohol and amine molecules is by one another.

4. CONCLUSIONS

In conclusion, under the same environmental conditions, the calculated and experimental values of binary mixtures in equilibrium for three 1-butylamine+alcohol system at two different temperatures 303.15K and 313.15K. The data shows that our results describe all excess functions ranging from positive values to strongly negative. The system exhibits very strong cross association through OH-NH_2 group. The values of viscosity of three binary mixture decreases with the increase in mole fraction of butyl amine at 303.15K. All three mixtures show strong negative deviation of viscosity and excess molar volume from the mole fraction of linearity. The magnitude of negative deviation rises with the chain length of alcohol, it is higher with heptanol than ethyl alcohol. while it decreases with the rise in temperature. The values of Gibb's energy of activation ΔG^{*E} for equiv. molar mixtures are positive, as the % of mole fraction of alcohol in amine increases, the viscosity and the density of the binary mixtures decreases at a particular temperature and is valid for all three mixtures. This decrease is slow for long chain alcohol+ butyl amine mixture at two temperatures. The variation in the values of excess molar volume deserve attention. With increase in concentration of alcohol in amines, the excess molar volume is high initially, but decreases gradually before attaining its original value. Contraction in volume is due to free volume difference of unlike molecules is due to hydrogen bond formation between amine and the alcohol through NH_2-OH and OH-NH_2 bonds This interaction can be considered as a reaction between the alcohol as a lewis acid and the amine as a lewis base.

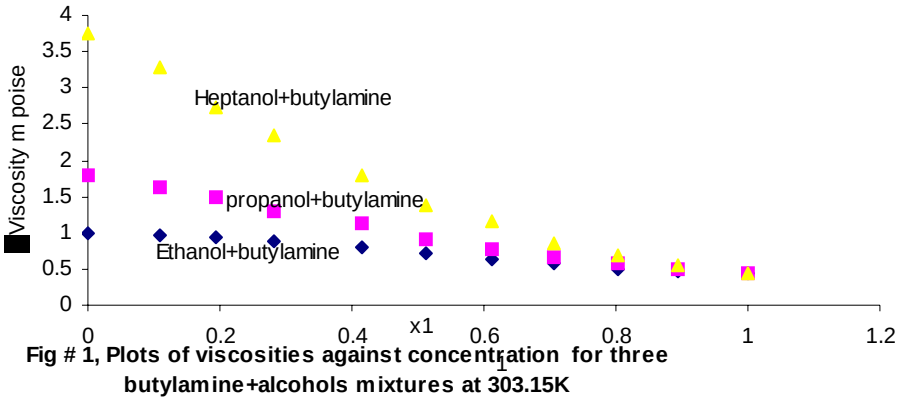

Fig # 1, Plots of viscosities against concentration for three butylamine+alcohols mixtures at 303.15K

Fig # 2, Excess molar volume V^E of three mixtures of Butylamine +alcohols at 303.15K

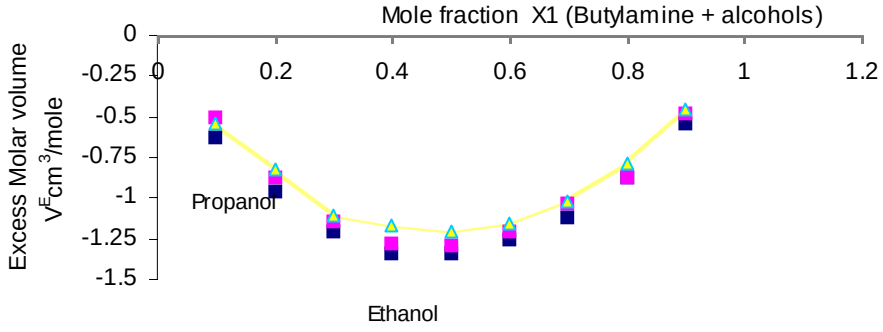

Fig # 3; Excess Gibb's Energy of activation ΔG^{*E} of viscous flow against concentration for three butylamine+alcohols mixtures at 303.15K

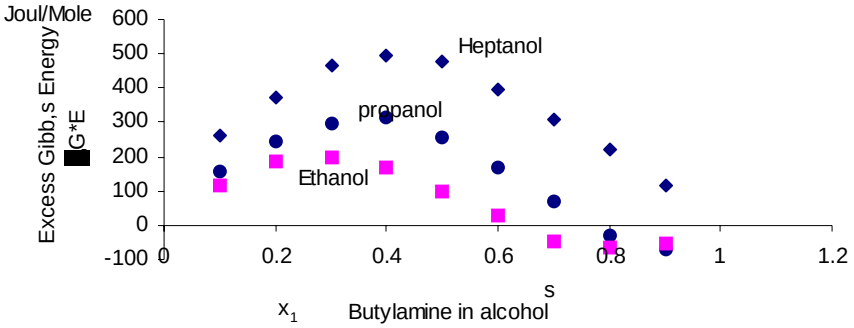

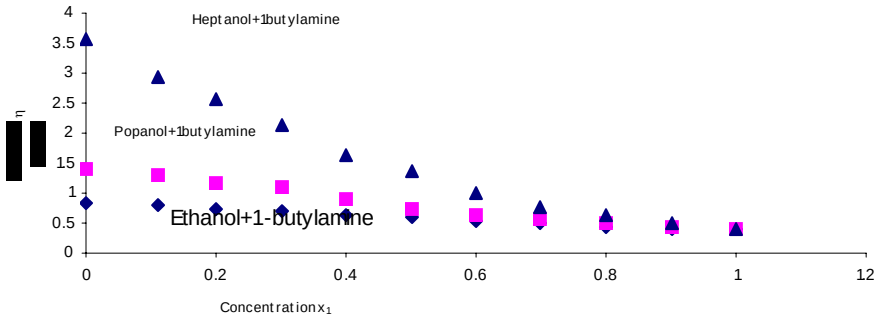

Fig; # 4; Plots of viscosity η against concentrations for the three mixtue of alcohols+1butylamine at 313.15K

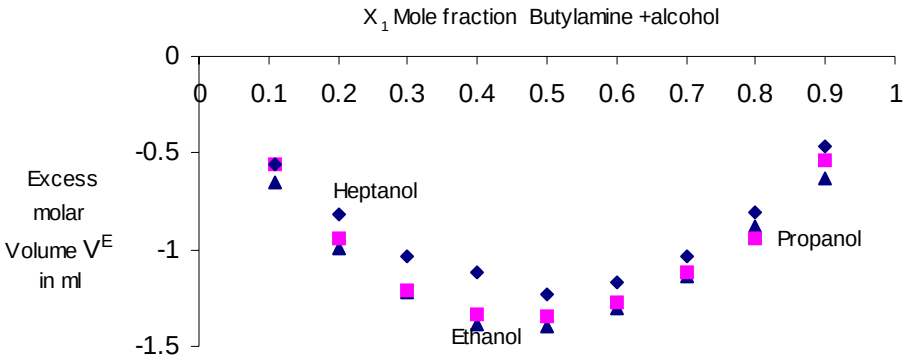

Fig# 5, Excess molar volumes (-ve Values) agaist concentration of Butylamine in alcohols at 313.15K.

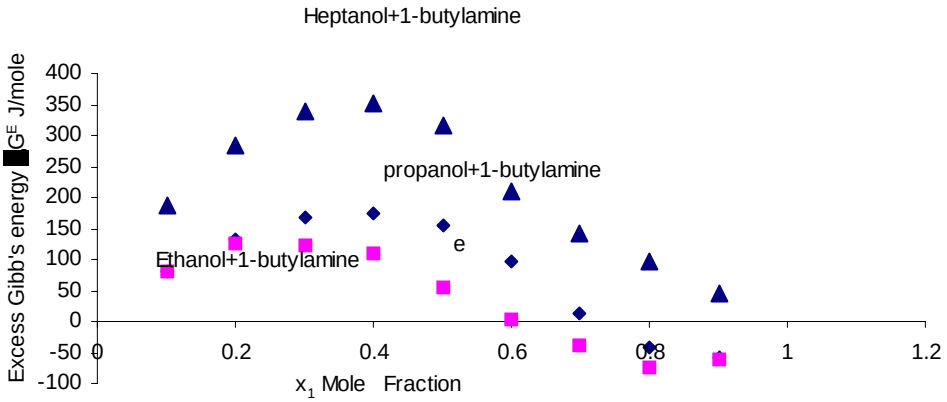

Fig: 6 Excess Gibb's Energy of activation ΔG^E of viscous flow for three 1-butylamine+alcohol mixtures at a temperature of 313.15K

REFERENCES

1. L.C Allen , 1975, A Simple model of Hydrogen bonding. J. Am. Chem. Soc. 97: 6921-6940.
2. Chandari, Shriang K, 2002," Vapour Liquid Equilibrium & Excess molar Volume of diethylamine+acetone and diethylamine +acetonitrile binary System" Fluid Phase Equilibrium
3. 200(2), 329-336.
4. Chibulka I. , Tamura K and Nagata I , 1988, 'Fluid phase Equilibrium' 39; 39-51
5. Liu Jiangue, Quin Zhang Feng Wang, 2002,' Liquid –Liquid Equilibria for methanol+water + Hexane ternary mixtures. ' J. of Chemical Engg data 2002 47(5)
6. Hedwig, Gavin R, Hakin Andrew W 2004, " The partial molar volume and heat capacities at infinite dilution for the electrolyte Tetraphenyl phosphonium chloride and sodium bromide in aqueous solution over the temperature range 298.15K -328.15K" J. of Physical Chemistry of Chemical physics 6(19), 4690-4700.
7. Prigogine L. 1967 'The molecular Theory of Solutions', Published by North Holland Publishing Co. N.Y, 55-66
8. Hilderbrand JM and Prausnitz J 1970, 'Regular and related solution theory'. Von Nostrand Reinhold Publishing Co. New.York pp-341-354.
9. Reiman R. . and A. Heintz 1991, 'Thermodynamic properties of mixtures." Proc. of Indian Acad. of Science (Chemical Soc). 20: 29-37.
10. Glastone S . K.J. Laidler, and H. Erying, . 1941,' Theory of rate process'. McGraw Hill Co. New York , 513-514.
11. 10. Quin A.W , D.F Hoffman and P. Munk. 1992 ' Excess Functions in Chemistry'
12. J. Chem Engg. Data. 37: 55-61.
13. S.D. Pradhan . 1981, Properties of aliphatic amines and their mixture. Proc .of Indian Acad. of Science , Chem. Soc. 90: 261-273.
14. Oswal S.L. .and H.S Desai 1998, ' Fluid Phase Equilibrium'. J .of Chem. Engg. Data,
15. 149: 359-376
16. Tanaka R , S. T. Oyama . and S. Murakami 1986, Solubility of alcohols in amines. J. Chem. Thermodynamics 18: 63-73.
17. Funke. H. Wetzel M. and Heintz A , 1989, New Applications of ERAS model . Thermodynamics of amines + alkanes and alcohol+amine mixtures. J. Pure & Applied Chemistry. 61(8), 1429-1439.
18. Nikiforov M, Aliper G.A and G.A Krestov . 1988, 'Calculations of the viscosity of binary liquid mixtures'. Zh.Fix Khim J. of USSR, 62,2:561-564.
19. F. Ratkovics and M. Laszlo, 1973, ' Properties of mixture containing amines and alcohol. and Thermodynamic properties of butylamine and butyl alcohols mixture'.Acta Chim Acad. Sci. Hung, 79 ,4: 395-400.

20. Martinaz, Santiago, Garriga, Rosa, Perez, Pascual Grocia, Mariano, 2000, 'Densities & Viscosities of Binary Mixtures of butanenitrile with Butanol isomers at several temperatures'. J. Chem. Engg. Data 45 ,6: 1182-1188.
21. Nikos T , G. Polowlogou and M.Maria 2000, ' Densities and Viscosities of 1-pentanol and Heptanol with Alkane binary mixtures at 293.15K'. J.of Chem .Engg. Data. Am. Chem. Soc. 45, 2: 272-275.
22. G.T. Gao, J.B. Woller ,X.C Zeng and W.Wang W 1997, 'Solute-Solvent size ratio dependency of the solute residual chemical potential in subcritical solvents'. J. Mol. Phy. 90(1) 141-146.
23. Mikio T and Michio K 1952, 'On the viscosity of binary liquid mixtures' .Bull. of Chem. Soc. Japan 25: 32-40.
24. Musai, Lelia, Postigo, Mirguel and Charles R, 2001, 'Viscosity Measurements for binary mixtures of 1,2 Dichloro-ethane with 1,2 Dibromoethane with isomeric butanol. J.of Chem Engg. Data, 45:86-91 .
25. Grunberg L. and A.H. Nissan A.H, 1949,'Mixture law for viscosity' Nature, 164: 799-800
26. Flory P.J , R.A. Orwoll . and A.Vrij 1964, 'Statistical Thermodynamic of long chain molecules in liquid, an equation of state for the normal paraffine Hydrocarbons'. J. Am. Chem. Soc. 86: 3504-3520.
27. Davis , Michael I, Molina M, Concepeion, Donheret Gerard, 1988, " Excess molar volumes and excess enthalapies of the 2-butyl oxyethyanol+water system at 25^0C' .
28. Thermodynamic Chim Acta , 131:153-170.

PK ISSN 0022- 2941; CODEN JNSMAC
Vol. 46, No.1 & 2 (April & October 2006) PP 33-38

GAMMA IRRADIATION EFFECT ON YBCO AND (Bi, Pb)SCCO HIGH TEMPERATURE SUPERCONDUCTORS

K.M. Bhutta*, S. Ali*, S. A. Siddiqi**
*Department of Physics, G.C. University, Lahore-54400, Pakistan.
**Centre for Solid State Physics, Punjab University, Lahore-54590, Pakistan.
salamat601@yahoo.com

(Received: September 7, 2006)

ABSTRACT: The gamma irradiation effect on the YBCO and BiSCCO systems of HTSC are presented in this paper. $YBa_2Cu_3O_{7-\delta}$ and $(Bi_{1.8}Pb_{0.2})_2 Sr_2 CaCu_3 O_y$ superconducting samples were fabricated locally. The systems were characterized by measuring resistance using four probe method and structural analysis was performed using XRD. Samples were irradiated for different doses of gamma irradiations. An increase in T_{CO} was observed in initial small doses of irradiations. Further increase in T_{CO} was observed when sample of YBCO was exposed to gamma radiations in steps of 2.5 Mrad. But a decrease in T_{C0} and $T_{c\ onset}$ was observed in BiSCCO system. This pointed that gamma rays induced some structural changes in HTSC. The (Bi, Pb)SCCO system showed the effect of gamma irradiation in different manners as compared to that of YBCO.

1. INTRODUCTION

The present work is a report on the effect of various doses of gamma irradiation on $YBa_2Cu_3O_{7-\delta}$ and $(Bi_{1.8}Pb_{0.2})_2Sr_2CaCu_3O_y$ superconductors. Quite different and contradictory results about the effect of gamma irradiation on the properties of YBCO and (Bi, Pb)SCCO are found in literature. Bohandy et al [1] reported that gamma radiation up to a dose of 1.3 MR has virtually no effect on the superconducting properties of YBCO. On the other hand Vasek et al [2] observed a noticeable increase in both Tc and normal state resistance of $Y(Sm)Ba_2Cu_3O_{7-\delta}$ with gamma irradiation. Boiko et al [3] observed a drop of T_C in $Y_{0.9}Sm_{0.1}Ba_2Cu_3O_{7-\delta}$ at low gamma radiation dose and then a gradual increase of Tc of the same sample at high dose of gamma irradiation. On the other hand Kato et al found no significant change in Tc and normal state resistance of YBCO under gamma irradiation up to a dose of about 100 MR. Kutsukae et al [5] also concluded that there was virtually no change in Tc and resistivity of YBCO upon gamma irradiation up to 1000 MR.

2. EXPERIMENTAL SETUP

Two samples, marked 1 & 2, of $YBa_2Cu_3O_{7-\delta}$ were fabricated using conventional Solid State Reaction method. For $YBa_2Cu_3O_{7-\delta}$ fine powders of Yttrium Oxide Y_2O_3, Barium Carbonate $BaC0_3$, and Copper Oxide CuO were mixed in the composition of $YBa_2Cu_3O_{7-\delta}$ and ground in a mortar for half an hour. The mixture was calcinated in air at 950°C for about 24 hours. For intermediate firing the mixture was again heated in furnace at 950°C for about 24 hours. After pellets formation at the pressure of 10 Pa, the samples were heated third time at 950°C for 24 hours. During all heat treatments the furnace was programmed to reach at the temperature of 950°C in one hour and remained at that temperature for 24 hours followed by cooling down to 500 ^{0}C degrees at the rate of 100 ^{0}C/hour then to room temperature at the rate of 200°C/hour.

Two samples, marked 3 & 4, with nominal composition of $(Bi_{1.8}Pb_{0.2})_2\ Sr_2\ CaCu_3O_y$ were also fabricated by solid state reaction technique. The starting materials were fine powders of Bismuth Oxide (Bi_20_3), Lead Oxide (PbO), Calcium Carbonate ($CaC0_3$), Strontium Carbonate ($SrC0_3$) and Copper Oxide ($Cu0_3$). These powders were mixed and ground for half an hour. The heat treatment of $(Bi_{1.8}Pb_{0.2})_2\ Sr_2\ CaCu_3O_y$ is similar to that explained above. The difference is the temperature and time of heating the sample. In this sample the final temperature during the first heat treatment is 750 ^{0}C for 24 hours and during the last heat treatment is 850°C for 100 hours. In these samples intermediate firing is not carried out and rate of cooling is not important.

The resistances versus temperature of the samples were measured by Four Probe Method. These measurements were made on both freshly prepared and irradiated samples. X-ray diffraction analysis of the samples was carried out using PANalytical X'pert Pro- X-ray diffractometer using CuKα radiation obtained through Ni Filter at room temperature. The irradiation process was carried out at Pakistan Radiation Service (PARAS) by Co-60 gamma source.

3. RESULTS AND DISCSSIONS

For this study two samples each of $YBa_2Cu_3O_{7-\delta}$ and $(Bi_{1.8}Pb_{0.2})_2\ Sr_2\ CaCu_3O_y$ were fabricated under the same conditions and are, therefore, supposed to be similar in structure. One of the each samples were converted into powder for XRD analysis and their results are shown in Fig.l and Fig.2.

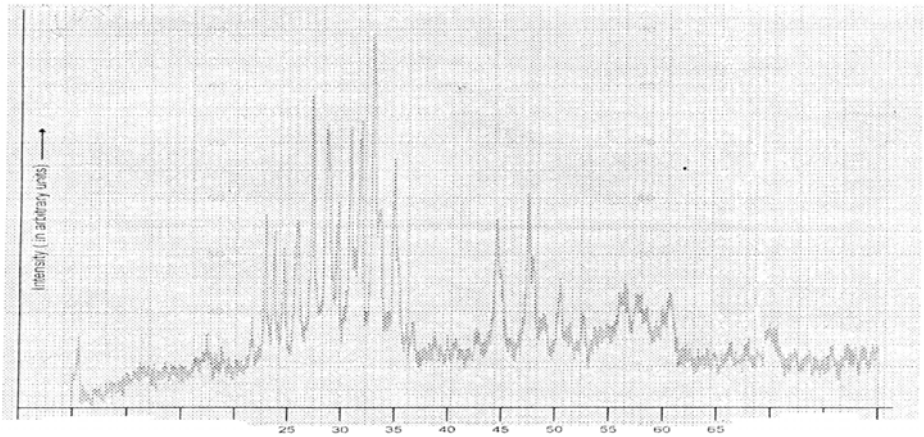

Fig. 1. XRD-Pattern of $YBa_2Cu_3O_{7-\delta}$ before γ - irradiation.

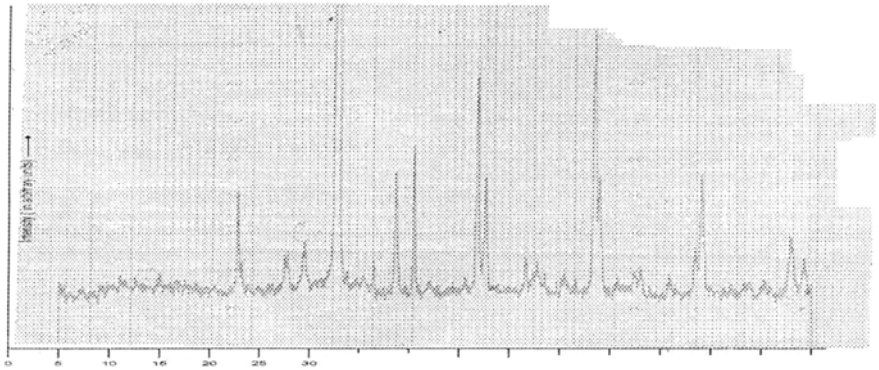

Fig. 2. XRD Pattern of (Bi, Pb)SCCO before γ - irradiation

Other samples 2 and 4 were irradiated by γ-rays for three different doses each of 2.5 MR. In case of $YBa_2Cu_3O_{7-\delta}$ an increase in Tco values after each dose of irradiation has been observed as shown in Fig.3. In case of (Bi, Pb)SCCO an increase in Tco value after first 2.5MR dose of irradiation and then a decrease in Tco value has been observed as shown in Fig. 4.

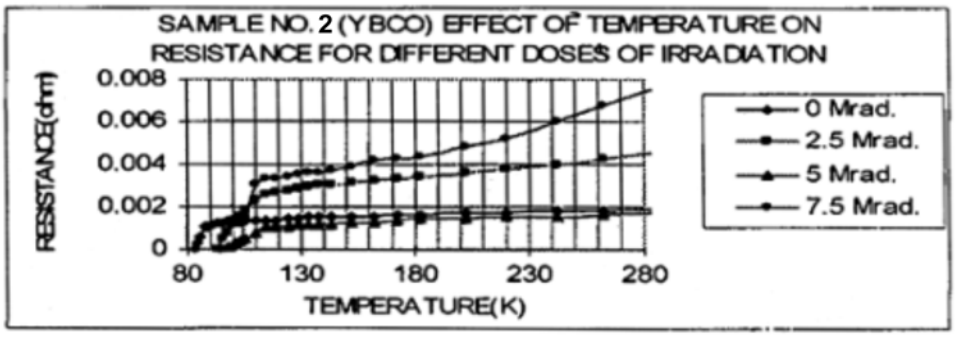

Fig. 3. Effect of temperature on resistance of $Yba_2Cu_3O_{7-8}$ for different doses of γ irradiation.

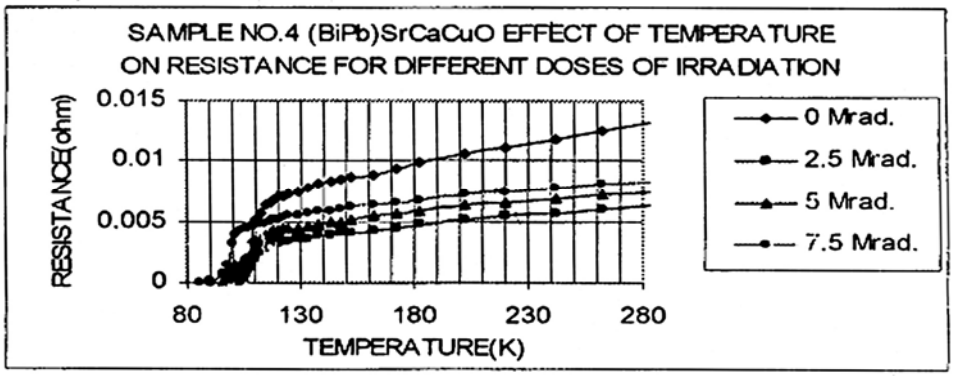

Fig. 4. Effect of temperature on resistance of $(Bi_{0.8},Pb_{0.2})2SrCaCu3Oy$ for different doses of γ irradiation.

In order to explain the results, it must be realized that both the compositions YBCO and Bi(Pb)SCCO have shown a relatively lower Tco values of 83.3K and 93.3K respectively. These lower values indicate that the samples are not homogeneous and their XRD patterns also indicate that they are multiphase. With such micro-structural characteristics, it is expected that the superconducting grains are relatively large volume of grain boundary areas providing a poor conduction between these grains.

It is observed that irradiation has increased the Tco values of such a YBCO sample. The degree of increase in Tco values after each irradiation step of 2.5 MR was, however not of same value. Maximum increase in Tco value 10 K was observed after first dose of irradiation. In the subsequent irradiation the increase in Tco were 2K and 6K respectively as shown in Fig. 5. The grain boundaries in YBCO are oxygen deficient and disorder regions [6,7]. Tco of the oxygen deficient regions increases by the change of charge carrier density. The most important effect of γ-rays in solid is ionization. It is suggested [8] that gamma irradiation can generate electrons holes pair in CuO_2 planes. Electrons can be brought far away from their initial place due to the high energy of gamma rays and trap there, while holes remain mobile in CuO_2 planes. This should increase the charge carrier density in the plane and therefore enhance the Josephson coupling between the adjacent grains. If this takes place in some of weak links then this will result in increasing of Tco.

For YBCO the Tco value increased to 95.25 K but T_{conset} remained at 114K on exposing the sample with 5MR. At the dose of 7.5 MR the Tco increases to 101.3K but T_{conset} remained at 114K as shown in Fig. 3. It means that the coupling link improved by the increase of dose of irradiation at the temperature near to the Tco.

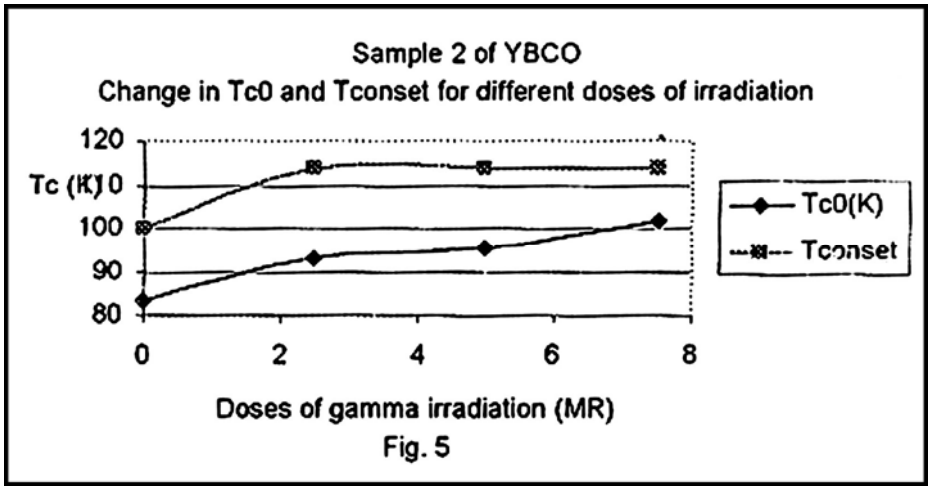

Fig. 5

The $(Bi_{0.8}Pb_{0.2})_2Sr_2CaCu_3O_y$ also showed the effect of γ-irradiation but in a different manner as compared to that of YBCO sample as shown in Fig. 6.

The sample showed Tco equal to 103.3K and T_{conset} at 120K after first dose of irradiation of 2.5MR. Foot of the curve was disappeared and curve became smooth after 2.5MR of irradiation. It means that coupling become strong between the grains and the crystal showed single phase character. By further irradiating the sample the foot appeared again and a decrease in Tco was observed due to disordering effect of γ irradiation. Smoothness of curve shows that this was done only at temperature near the critical temperature. All these results are shown in the Fig. 4 and Fig. 6.

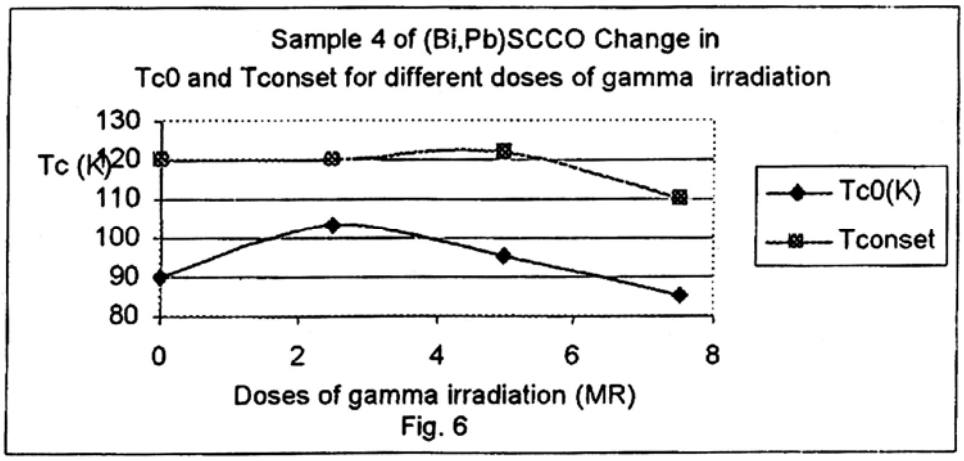

Fig. 6

At the irradiation of dose of 7.5 MR the foot of the curve become sharp and the transition from the normal to superconducting state become narrow as shown in Fig. 4. A decrease in Tco and T_{conset} was also observed at 7.5 MR.

The increase in Tco in $(Bi_{0.8}Pb_{0.2})_2Sr_2CaCu_3O_y$ may be due to ionization effect of gamma irradiation [8] and Tco reaches to an optimum value of 103.3K. After reaching a value of 103.3K a decrease in Tco has been observed. This may be explained by the disordering effect of γ - rays which deplete charge carriers in the region of grain boundaries thus breaking the current carrying chain between the grain boundaries and weak Josephson coupling link. At the high doses in $(Bi_{0.8}Pb_{0.2})_2Sr_2CaCu_3O_y$ disordering effect overpower the ionizing effect of γ -rays.

4. CONCLUSION

It may be inferred that understanding of γ rays influence is far from completion and therefore further experimental and theoretical investigation of this matter are necessary.

5. REFRENCES

1. **Bohandy, 1. Suter, b. R. Kim, K. Moorjan, and F. 1. Adrian, Appl. Phys. Lett. 51(1987) 2161.**
2. **P. Vasek, L. Samreka, 1. Dominee, and M. Pesek, Solid State Commun. 69 (1989)23.**
3. **B.'B. Boiko, F. D. Korshunov, et al, Phys Status Solidi (a) 107 (1988) k139.**
4. **T. Kato, M. Watanabe, Jpn. 1. Appli. Phys. 27 (1988) L2097.**
5. **T. Kutsukae, H. Somi, Jpn. 1. Appli. Phys. 28 (1989) L1393.**
6. **V. S. Boyko, 1. Malinsky, N. Abdellatif, and V. V. Boyko, Phys. Lett. A 244 (1998)561.**
7. **S. V. Stolbov, M. K. Mironova, and K. Salama, Preprint No. 98: 128, Texas Center for Suerconductivity at the University of Huston.**
8. **B. I. Belevtsev, et al, Effect of irradiation on superconductivity in Polycrystalline $YBa_2Cu_3O_{7-\delta}$, arXiv: cond-matt/007345 v1, 21 Jul 2000.**

PK ISSN 0022- 2941; CODEN JNSMAC
Vol. 46, No.1 & 2 (April & October 2006) PP 39-46

TO STUDY THE CORRELATION BETWEEN MICROSTRUCTURE AND MECHANICAL PROPERTIES OF AL-MG-CR ALLOY AFTER WORK HARDENING

M. N. Ishaq, S. T. A. Shah*, S. Ali
Dept. of Physics, GCU. Lahore, Pakistan
* Centre for Advanced Study of Physics, GCU. Lahore, Pakistan

(Received: September 13, 2006)

ABSTRACT The effect of cold-work and heat treatment on the microstructure development and changes occurred in the mechanical properties of Al-Mg-Cr alloy has been studied at large. The samples were homogenized at 573 K for one hour and allowed to cool at room temperature. X-ray fluorescence spectroscopy (XRF) was employed to ensure the exact elemental composition of the alloy. The samples were cold worked under normal static load of 30 KN with time variation to get 1% to 7% reduction in thickness. After work hardening the samples were aged for four hours at 373K. Optical microscopy was used to study the microstructure. Vickers hardness test was carried out to study hardness, which was improved as a result of work hardening. The steady state creep rate was found to be decreased as a result of above-mentioned treatment.

1. INTRODUCTION

Aluminum- Magnesium- Chromium is a non-heat treatable alloy [1-2] that is generally known for its excellent corrosion resistance. The Al-Mg-Cr alloys have a wide range of strength, good forming and welding characteristics, and high resistance to corrosion as has been shown by Haszler et. al. [3]. The work of Gholinia, et. al. [4] showed the conditions under which micron-scale structure can be developed in Al-Mg-Cr alloy. The Niikura, et. al. [5] related with the refinements of recrystallized grain and its effects on mechanical properties in Al-Mg alloys. For the purpose of obtaining aluminum P/M materials strengthened by solid solution of Mg and dispersion of transition metal compounds, Fujii, et. al. [6] worked on rapidly solidified Al- Transition metals with addition of Mg Rapid solidification (RS). Jian et. al. [7] Investigated the influence of chemical composition on the microstructure and mechanical properties of Al Mg alloys. The work of Taleff, et. al. [8] showed that the solute-drag creep was observed in many aluminum alloy containing magnesium concentration from as little as 2 wt%, to the limit of solubility. Kaigorodeva [9] worked on microstructure and mechanical properties evolution during long term aging of Al-Mg alloy by optical and transmission electron microscopy as well as tensile test and corrosion resistance decreased during aging which result from film like grain boundary B' and β phase precipitation. The work reported by Savas et. al. [10] covered a comparative investigation of the Aluminum-Magnesium cast alloys containing up to 10% Mg.

To our knowledge, not a lot of work has been done to find the correlation between microstructure development and the changes occurred in mechanical properties of Al-Mg-Cr alloy after cold work. To find the correlation, pre-prepared Al-Mg-Cr alloy was subjected to study with reference to the mechanical properties and microstructure development as a result of cold work followed by aging.

The paper has been divided into four major sections followed by many sub-sections. Section 1 introduces the field and what major work has been done until now in this field. Section 2 describes the sample preparation steps. While the section 3 provides the results of research completed here followed by the comprehensive discussion including elemental analysis, optical microscopy, creep studies, effect of work hardening on steady state creep rate, and the hardness studies. The fourth section concludes the work.

2. EXPERIMENTAL SET-UP

As stated above, to find the correlation between microstructure and mechanical properties of Al-Mg-Cr alloy, the pre-prepared Al-Mg-Cr alloy was subjected to cold work followed by aging. For this purpose seven samples were prepared. The elemental composition was determined using x-ray fluorescence spectrometer (XRF). The samples were homogenized at 573 K in an electric furnace for an hour and allowed to cool at room temperature. These samples were cold worked from 1% to 7% reduction in thickness under normal static force of 30 kN in isothermal condition. After cold working, the samples were aged for 4 hours at 373 K. Optical microscopy was used to study the microstructure of properly etched samples. Vickers hardness test and creep test were carried out to investigate the mechanical properties of the samples.

3. RESULTS AND DISCUSSION

3.1. ELEMENTAL ANALYSIS

The material under study was an Al-Mg-Cr alloy system. After having x-ray fluorescence spectrometry for the elemental analysis the principal composition of the alloy comes out to be as shown in Table.1

Element	Al	Mg	Cr	Mn
Wt. %	94.65	4.8	0.1	0.2

Table 1: Elemental analysis of the principal composition of the Al-Mg-Cr Alloy based upon XRF.

3.2. OPTICAL MICROSCOPY

The microstructure of the Al-Mg-Cr alloy has been examined by optical microscope. The optical micrograph of the samples of alloy is shown in Fig.1 - Fig. 7.

Fig.1 & Fig 2 are the micrographs of Al-Mg-Cr alloy samples subjected to work hardening form 1% & 2% under normal static force of 30 kN and heat treated at 373 K, respectively. Two types of species can obviously be seen. Firstly the lighter gray equiaxed precipitates with coarse grain boundaries constituting the host matrix. Their average grain size lies in the range 30 μm ~ 170 μm. Secondly black precipitates of smaller size are observed. These precipitates are irregular in shape and size and are randomly distributed over the matrix at grain boundaries and within a grain. Almost no significant change of microstructure is observed in sample with 2% work hardening.

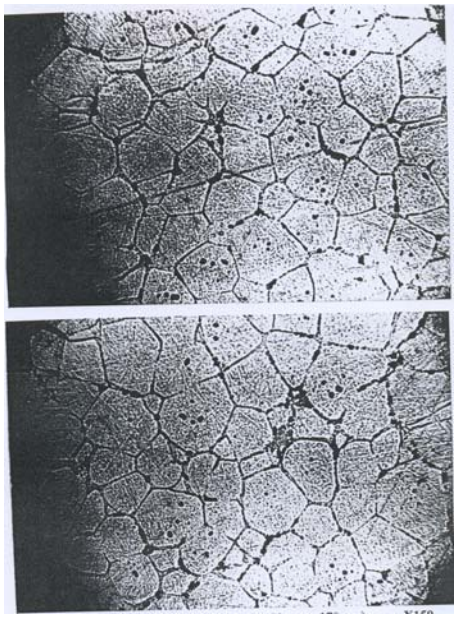

Fig. 1&2: (Average Grain size 30 μm ~ 170 μm), Magnification: 150 , Micrograph of Al-Mg-Cr alloy work hardened from 1% & 2% under normal static force of 30kN and heat treated at 373 K.

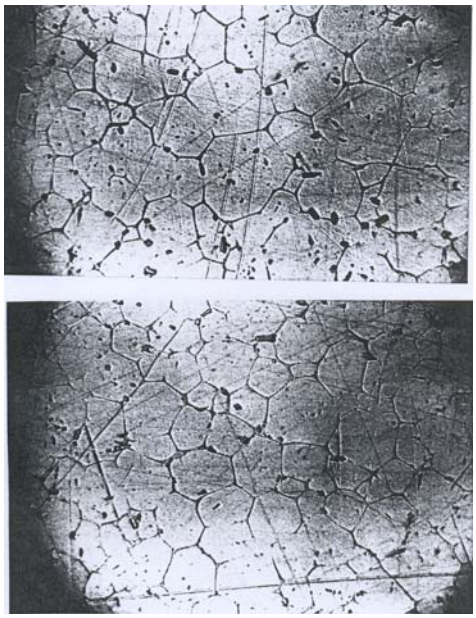

Fig. 3&4: (Average Grain size 22 μm ~ 145 μm), Magnification: 150 , Micrograph of Al-Mg-Cr alloy work hardened from 3% & 4% under normal static force of 30kN and heat treated at 373 K.

Fig.3 & fig 4 are the micrographs of Al-Mg-Cr alloy samples subjected to work hardening form 3% & 4% under normal static force of 30 kN and heat treated at 373 K, respectively. Equiaxed grains with average grain size in

the range 22 µm ~ 145 µm are observed indicating slight grain refinement as a result of cold work. Black precipitates are seen to be segregated at grain boundaries resulting in decease in population of these precipitates within the grains. Furthermore, minor refinement of the grain boundaries is also observed in sample with 3% & 4% work hardening.

Fig.5 & fig .6 are the micrographs of Al-Mg-Cr alloy samples subjected to work hardening form 5% & 6% under normal static force of 30 kN and heat treated at 373 k, respectively. Equiaxed grains with average grain size in the range 20 µm ~ 140 µm are observed. Significant grain refinement as a result of cold work is observed in these samples. Black precipitates segregation and growth at grain boundaries resulting in decease in population of these precipitates within the grains is observed in these micrographs. It is also observed that the black precipitates have attained small circular palette shapes and have become significant within the grains. It is obviously observed that the microstructure of the Al-Mg-Cr alloy has been refined and there is significant grain boundaries refinement in sample with 5% & 6% work hardening.

Fig.7 is the micrograph of Al-Mg-Cr alloy sample subjected to work hardening form 7% under normal static force of 30 kN and heat treated at 373 k, respectively. Equiaxed grains with average grain size in the range 20 µm ~ 135 µm are observed. No significant micros rural changes are observed in this sample. It indicates that the grain size has attained a saturation state i.e. grain size has turned almost insensitive to work hardening. Negligible refinement in the grain boundaries is observed in this sample.

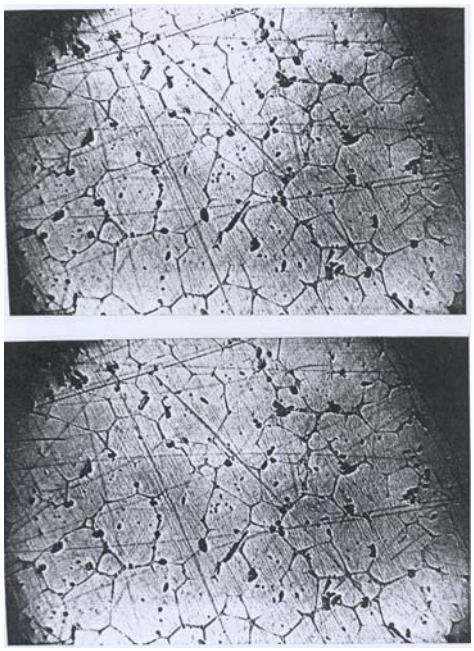

Fig. 5&6: (Average Grain size 20 µm ~ 140 µm), Magnification: 150 , Micrograph of Al-Mg-Cr alloy work hardened from 5% & 6% under normal static force of 30kN and heat treated at 373 K.

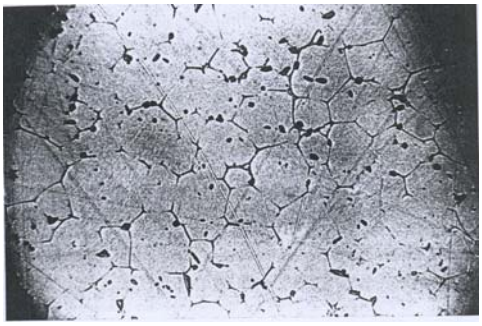

Fig. 7: (Average Grain size 20 µm ~ 135 µm), Magnification: 150 , Micrograph of Al-Mg-Cr alloy work hardened from 7 under normal static force of 30kN and heat treated at 373 K.

3.3. CREEP STUDIES

The creep test on the Al-Mg-Cr alloy has been performed at constant stress of 100 MPa and temperature of 493 K for 12 hours. The Fig.8, shows the combined plot of creep curves of all the seven Al-Mg-Cr alloy subjected to work hardening from 1% to 7% under normal static force of 30 kN and heat treated at 373 K .

All the samples have similar creep behavior except the sample with 4% work hardening. The only and the most important difference in the creep behavior of all Al-Mg-Cr alloys is that of creep deformation rate. The creep studies, carried out for 12 hours at 493 K ± 1% and 100 MPa revealed that the steady state creep rate (SSCR) of all the samples lie in the range 0.0080 µm / sec. ~ 0.0155 µm / sec.

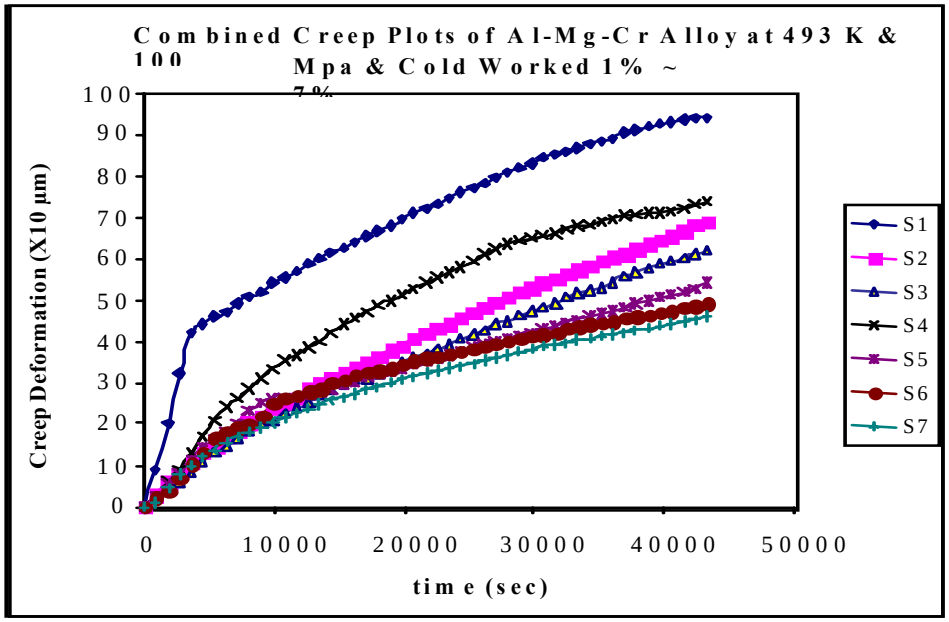

Fig. 8: Combined Creep Plots of Al-Mg-Cr alloy at 493 K, 100Mpa, Cold Worked 1 –7%.

S. NO.	COLD WORK (%)	SSCR (µm / Sec)
1	1	0.0155
2	2	0.0146
3	3	0.0128
4	4	0.0131
5	5	0.0093
6	6	0.0083
7	7	0.0080

Table 2: Effect of % Cold Work on Steady State Creep Rate

3.4. EFFECT OF WORK HARDENING ON STEADY STATE CREEP RATE

The steady state creep rates (SSCR) of all the samples were worked out. The plot of steady state creep rate versus the aging time is shown in Fig. 9. The SSCR decreases, in general with increasing work hardening, shows a little increase for sample with 4% work hardening, and then decreases at a very small rate. The steady state creep rate lies in the range 0.0080 µm/sec ~ 0.0155 µm/sec. It is observed that minimum steady state creep rate comes out for samples with 6% & 7% work hardening and afterward it

seems to be less sensitive to work hardening. However the overall creep deformation of the sample with 7% cold wok comes out to be minimum.

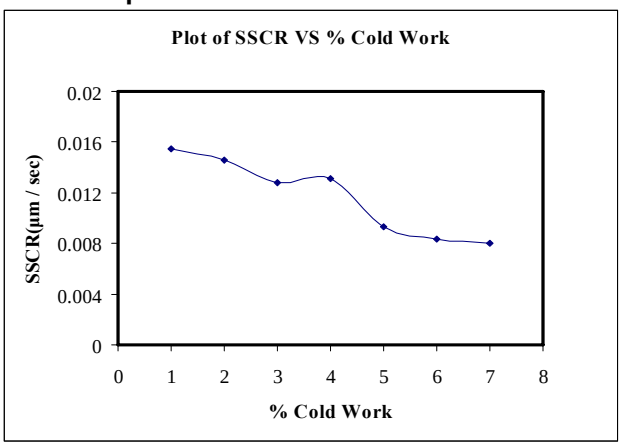

Fig. 9. SSCR Vs. % Cold work.

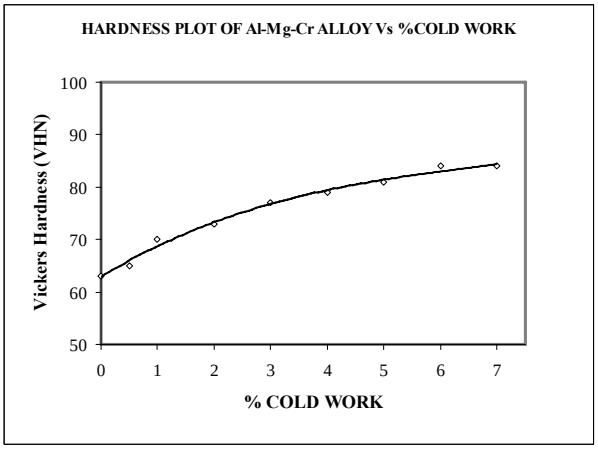

Fig. 10. Vickers Hardness Vs. % Cold work.

3.5. HARDNESS STUDIES

The Vickers hardness plot is shown in Fig. 10. (the effect of work hardening of Al-Mg-Cr alloy subjected to work hardening form 1% ~ 7% under normal static force of 30 kN and heat treated at 373 K, lying in the range 70 ~ 84 VHN.

The Vickers hardness in the initial part of hardness plot rises with work hardening with a higher rate and achieves steady state after 4% work hardening of the samples. The maximum Vickers hardness comes out for samples with 6% & 7% cold work.

4. CONCLUSION

It is concluded that the work hardening carried out on Al-Mg-Cr alloy affect the microstructure and mechanical properties. It is observed that the microstructure and mechanical properties are more sensitive towards work hardening for initial stages of cold work. Afterwards these effects become less sensitive towards work hardening.

REFERENCES

1. **W.D. Callister Jr, Material Science and Engineering, An Introduction, 6th Edition, John Wiley & Sons, Inc. 2003.**
2. **Smith W.F., "Principles of material science and engineering" 3rd edition, McGraw Hill, London 1996.**
3. **Haszler, A. J.P and Sampath, D. PcT Int. Appl. wo 99 42,(1998) 627.**
4. **Gholinia, A; Humphreys and Prangnell, P.B; Acta Materialia. 50, Issue 18, (2002) 4461-4476,**
5. **Niikura, A; Bekki, Y. Mater. Science forum 331-337 Trans Tech Publications Ltd, 2000.**
6. **Fujii, H; Sugamata, M; Kaneko, J; Kubota, M; and Keikinzoku, 50 (7) (2000) 330-334.**
7. **Jiang, D.M; Kang, S.B and Kim, H.w 10M communication Ltd. Material science and Technology, 15 (12) (1999)1401-1407.**
8. **Talefl, E.M; Navland, P.J; and Yoon, Sean, J. Deform; Process; prop. Struct. Mater; Proc. Honorary symp. Professor Oleg D. Sherby, (2000)373-384,**
9. **Kaigoradova, L.L Mater; Sci forum, (1999) 294-296.**
10. **Saras, M.A.; Altintas, S. Adv. Alum. Cast. Technol., Proc. Mater. Solution com. 98 (1998) 265-269.**

PK ISSN 0022- 2941; CODEN JNSMAC
Vol. 46, No.1 & 2 (April & October 2006) PP 47-51

A COMPARISON OF THE TRANSMISSION LOSSES OF DIFFERENT OPTICAL FIBER MATERIALS

S F SHAUKAT, M A U KHAN, R FAROOQ*
Department of Electrical Engineering,
COMSATS Institute of Information Technology,
Abbottabad, NWFP, Pakistan
E-mail: drsaleem@ciit.net.pk

*Department of Environmental Sciences,
COMSATS Institute of Information Technology,
Abbottabad, NWFP, Pakistan
E-mail: drubina@ciit.net.pk

ABSTRACT: A comparison of the optical losses and the quantum efficiencies of different types of optical fiber materials are discussed in this paper. Silicates, Heavy Metal Fluoride Glasses and now the Polymers are being used as the potential optical fiber materials. It has been revealed that a fiber with low transmission loss, high bandwidth, large core and low cost can be designed and fabricated using Polymethyl Methaerylate (PM). A minimum loss of 0.04 dB/m at 2.4 μm coupled with extended transparency beyond 5μm and excellent chemical stability makes these fibers potential candidate for infrared sensing, remote spectroscopy, laser power delivery and active fiber research.

1. INTRODUCTION

Silicates and Heavy Metal Fluoride (HMF) Glasses have been effectively being used as optical fiber materials since last decade and their significance cannot be ruled out. HMF fibers had been effectively being used in waveguides particularly in short range systems requiring sensing, active fibers and laser power transmission. These fibers had been acceptably stable with respect to devitrification but exhibited poor chemical durability and marginal mechanical strength. The capacity of optical fiber communications has expanded gigabits per second into terabits per second, enough the meet the current traffic demand due to the explosive growth of data transfer and internet services. In the area of fiber to the home or fiber to the premises application, passive optical networks especially ethernet passive optical networks and gigabit ethernet passive optical network are generally preferred for home connections. Usually the transmission bandwidth and transmission distance required for the networks are 100 MHz –10GHz and 100m–10 km respectively. Therefore, the fibers with lower loss, higher bandwidth and cheaper cost are in demand. Researchers have been trying to find materials and methods to meet those requirements and polymer optical fiber is one of the major approaches being explored. At present the most common polymer optical fiber material is Polymethyl Methaerylate (PM) that meet the current traffic demand, due to its intrinsic absorption loss mainly contributed by carbon-hydrogen stretching vibration in PM core [1-6].

2. EXPERIMENTAL RESULTS AND DISCUSSION

HMF glass fiber synthesis included fluorination and melting in platinum crucibles (1200ºC for core and 1100 ºC for cladding) under dry nitrogen glove box conditions. The HMF glass matrix contained the AlF_3, BaF_2, CaF_2, YF_3, SrF_2, MgF_2, NaF, ZrF_4 and PbF_2 with different concentrations of core and cladding. Following fabrication of a high optical quality cladding glass tube by rotational casting, the core glass was immediately poured into the cladding tube and cooled slowly. The preform size was 160mm length x 15mm diameter. The preform surface was mechanically polished and then chemically etched with a 0.5N solution of AlF_3 and HCl for about an hour at room temperature. Prier to drawing, the preform was also kept at 200 ºC for 2 hours while exposed to NF_3 to remove any residual water from the surface. Fiber drawing was accomplished using a resistance furnace with a localized heat zone of 20 mm in a tower enclosed by a unique three stage vertical glove box in which the moisture level was maintained below 1ppm. Typical drying speeds were in the range of 0.7m/minute with 150meters of fibers readily produced. Fiber dimensions were 120 µm for the core diameter with a 65 µm cladding thickness over-coated by a acrylate polymer. Perkin Elmer FTIR was used to measure the optical loss of the fiber by the cut – back technique. Figure 1 shows the comparison of the transmission losses of the Polymethyl Methaerylate (PM) fiber and the HMF based glass fiber. The minimum loss is 0.04 dB / m at 2.4 µm for PM fiber. This represents a significant advance in transmission losses. A major advantage of the PM fiber relative to heavy metal florides is the minimum transmission loss and excellent chemical durability. They have been survived in the laboratory for extended periods in boiling water in contrast to a few seconds for fluoride based fiber. They have also been used successfully for evanescent sensing in aqueous environment degradation [7}.

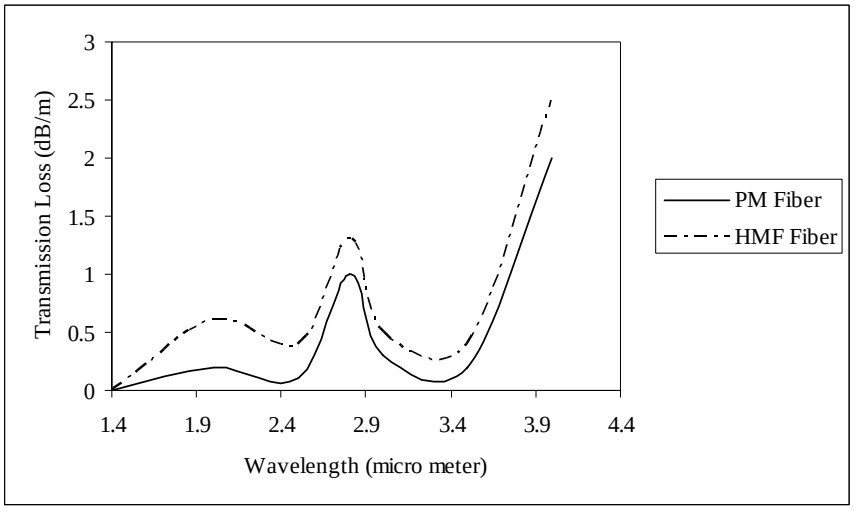

Figure 1: Transmission loss spectra of PM fiber and HMF fiber

3. 2-D FINITE DIFFERENCE TIME DOMAIN METHOD AND PLANE-WAVE EXPANSION METHOD

Optical properties of hollow-core fibers with cobweb cladding structure are analyzed by the compact 2-D finite difference time-domain method and the plane wave expansion method. A hollow-core Bragg fiber with and without supporting structure is analyzed with parameters as follows: n_1 = 1 (air), n_2 = 1.51 (refractive index of PM), d_1 = 0.75 μm, d_2 = 0.23 μm, A = d_1 + d_2 = 1.08 μm, r_{co} (Radius of the hollow core) = 9 μm, N (number of alternating layers) = 5 and operating wavelength λ = 0.85 μm (one of lower absorption loss windows for PM). The mechanical properties of hollow – core fibers with cobweb cladding structure are analyzed by the finite – element method. Structural parameters of the hollow–core fibers with cobweb cladding structures are d_1 = 1.5μm, d_2 = 0.35 μm, r_{co} = 18 μm, N = 6, number of supporting strips (m) = 9 and width of supporting strips (W_s) = 0.25 μm. The material is PM, whose elastic modules, Poison ratio and yield limit are 3.5 GPa, 0.43 and 65MPa, respectively. Taken the length of the fiber, l=2800 μm, the displacement load on the fiber is imposed at different radii of curvature. The relationship of maximum principal stress on the cross section with the radius of curvature after load is illustrated in Figure 2, for which the simulation is realized using ANSYS software [8-10]. When the outer diameter D_o is 500 μm, maximum principal stress will reach the yield limit. Flexural rigidity on the cross- section increases as the width of the supporting strips decreases.

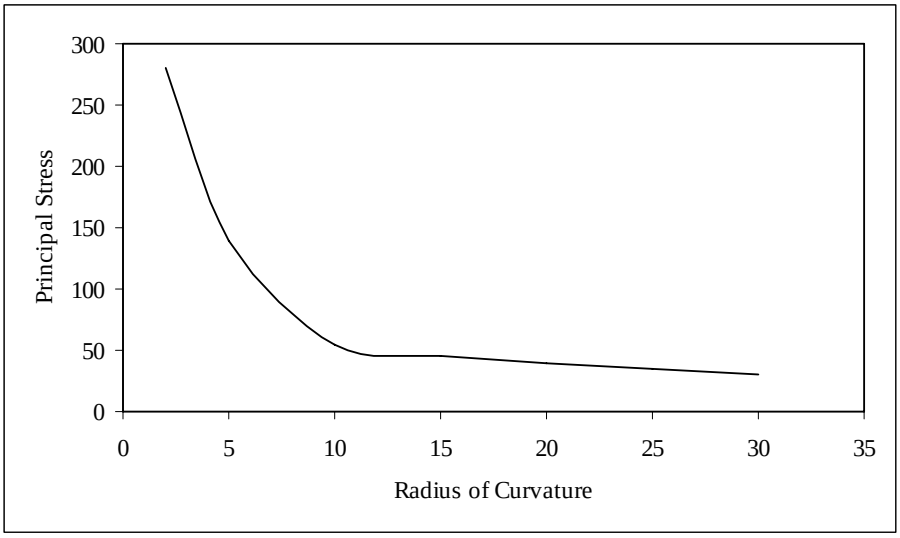

Figure 2: Relation curve of maximum principal stress with radius of curvature (ρ)..

To reduce the effect of supporting structure on transverse electric field, the number and width of supporting strips should be as small as possible, as long as the structures meet the requirements of mechanical stability.

The simulated results for structures have also proved these points. Figure 3 shows the leakage losses of the fibers with $\eta = (d_2/d_1) = 0.24$, $d_2 = 0.35$ µm and $n_2 = 1.51$ under different core radii at $\lambda = 0.75$ µm. As shown in figure 3 to achieve a lower leakage level, the number of alternating layes requires only 3–4. At $r_{co} = 10$ µm and N = 3 and 4, the leakage loss is 2.4×10^5 and 5.4×10^6 times larger than that of HMF mode respectively [11]. Therefore, depending on the model–filtering effect may realize the transmission of PM single mode or a few modes, thus achieving the transmission of higher bandwidth (GHz). The hollow–core fibers with larger core diameter are favorable for reducing both the leakage loss and connection loss between two fibers.

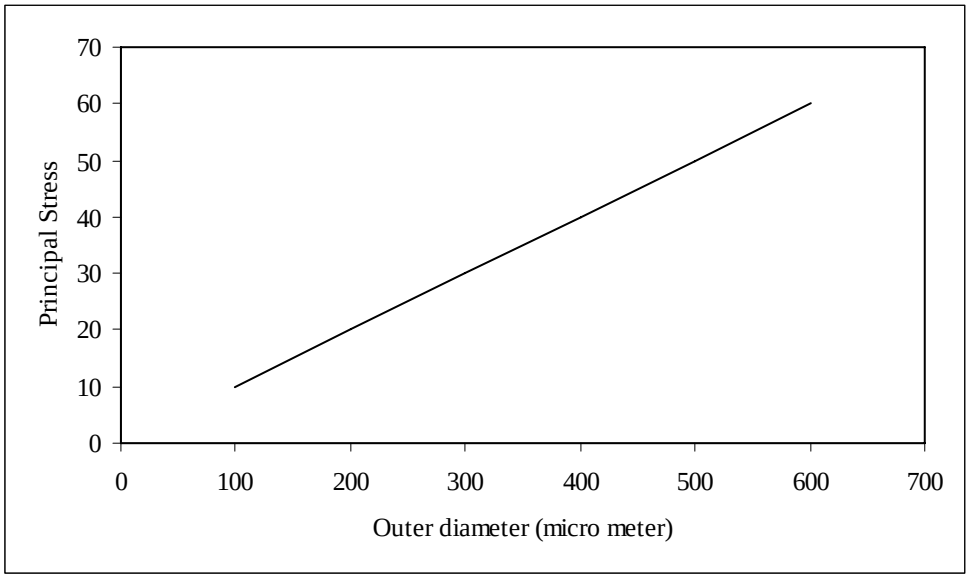

Figure 3: Relation curve of maximum principal stress with outer diameter (D_o).

4. CONCLUSIONS

A 50 fold reduction in the optical loss of PM fiber with the use of high purity material and by optimizing the melting, casting and drawing conditions have been achieved. A minimum loss of 0.04dB/m at 2.4 µm with expended transparency beyond 5 µm and exceptional durability makes these fibers excellent candidate for infrared sensing, remote spectroscopy, laser power delivery and active fiber application. The results show that after deducting the factors (material purity, imperfection and non uniformity of fiber structure and effect of supporting structure), a very board range of the wavelengths may be adopted for signal wavelength. Thus using a low-cost material (PM), it allows the fibers to meet the needs of the transmission distance and bandwidth to comprehend the wavelength division multiplexing.

REFERENCES

1. Y Koike, Giga-island, "Proc. Second Asia-Pacific Polymer Fiber Optics Workshop, Hong Kong, China, 2003.
2. A Argyros, M A Van, et. al., 'Hollow-core microstructure polymer optical fiber' in "The 14th International Conference on Polymer Optical Fiber", Hong Kong, China, 2005.
3. S G Johnson, M Ibanescu, et. al., "Opt. Express" 9, 748, 2001.
4. B Temelkuran, S D Hart, et. al., "Nature 420", 650, 2002.
5. A Argyros, N Issa, et. al., "Opt. Letters", 29, 20, 2004.
6. Kanamori T, Okawa K, et. al., "Japanese J. of Applied Physics", 20, 1236- 1240, 2002.
7. S F Shaukat, K J McKinley, P S Flower, P R Hobson, J M Parker, *J. Non-Crystalline Solids*, 244, 197–204, 1999.
8. M.A. Green, "Operating Principles, Technology and Systems Applications, Prentice Hall, NJ, USA, 2000.

PK ISSN 0022- 2941; CODEN JNSMAC
Vol. 46, No.1 & 2 (April & October 2006) PP 53-60

EFFECT OF ATMOSPHERIC CONDITIONS ON CABLE TERMINATION TO SWITCHGEAR

Abdur Rashid, Asmatullah Khan and S.F Shaukat
Department of Electrical Engineering,
COMSATS Institute of Information Technology Abbottabad

(Received : October, 09, 2006)

ABSTRACT: An intensive research work is carried out to determine the effect of humidity and contamination on cable termination and it's aging. In this paper, the effect of atmospheric conditions on cable termination has been investigated by measurement of discharge inception voltage, discharge magnitude, dielectric loss and capacitance of each phase of cable.
The three possible conditions i.e normal, wet and contaminated have been simulated in the laboratory. The deterioration is determined under simultaneous stress from applied voltage and contamination by measuring various parameters.
It can be stated with some confidence that above mentioned factor under these conditions will help to know about the conditions of termination and aging of the cable.
The cable was three phase Aluminum core XLPE cable and connected to switchgear through an epoxy resin bushing. Termination was made by heat shrinkable method.

1. INTRODUCTION

Cable termination to power system equipment is an essential part. For cable termination to work properly, it should be void free to avoid partial discharges. However it is also weakest point of the system, because it is exposed to atmospheric condition. The power cable insulation assume to be reasonable well and void free so that there will be no partial discharge. In the process of cable termination, there always the possibility that voids are created practically at the edge of the insulation shields. These voids cause partial discharge and deterioration due to electrical discharges within voids which may lead to failure of the insulation.

It is considered knowledge of partial discharges (PD) measurements constitute one of the most promising tool for the evaluation of localized defects and damages [1]. In the field of power cables, several condition assessment system based on PD measurement are available, each characterized by specific supply voltage wave shape, data acquisition and celebration philosophy.

The performances of several advanced cable diagnostic system have recently compared in the frame of an extensive investigation carried out in CESI laboratories and in representative field conditions, the relevance findings are reported. In all the system considered, great attention is focus

on defect location while little information is available about the origin of the defect and their consequent harmfulness [2].
A less precise but more intensive way to look at the phenomenon is to consider the transient change in capacitance between conductor and ground shield of the cable when the cavity goes from non conducting to conducting [3]. Obviously, the capacitance increases when cavity is conducting, which means that a current must flow down the cable to charge the additional capacitance and maintain constant voltage on the cable. This current flows through the impedance of the cable and generates voltage pulse which propagates down the cable [4, 5].

Dielectrics loss, discharge inception voltage and change in the capacitance are the factors which show the conditions and aging of the cables [6, 7]. These factors can easily be determined and analyzed with in manageable time. This paper summarized the data, observations and their analysis regarding these factors.

2. EXPERIMENTAL METHOD AND EQUIPMENTS

2.1. PROCEDURE

The experiment was carried out in three different environmental conditions i.e. normal, wet and contaminated. In normal condition the readings were recorded according to ambient temperature and humidity in the laboratory while for the wet and contaminated conditions, a chamber was build with PVC tubes, covered with plastic sheets. Water was spread by the help of two pumps (figure 1).

Water sprayed for six days and conductivity of water was 90 μs/cm and 600μs/cm for wet and contaminated conditions respectively.

2.2. TEST OBJECT

Test object was 11 kV three phase aluminum XLPE cable about 3 meters long and terminated to switchgear. The termination of the cable was made by using a heat shrinkable termination system. In termination process, care must be taken to avoid voids formation and also kept leakage current minimum. Phase to phase and phase to earth clearance should be such that there will be no flash over.

2.3 SALT-FOG CHAMBER

The schematic diagram of chamber is shown

Figure 1:

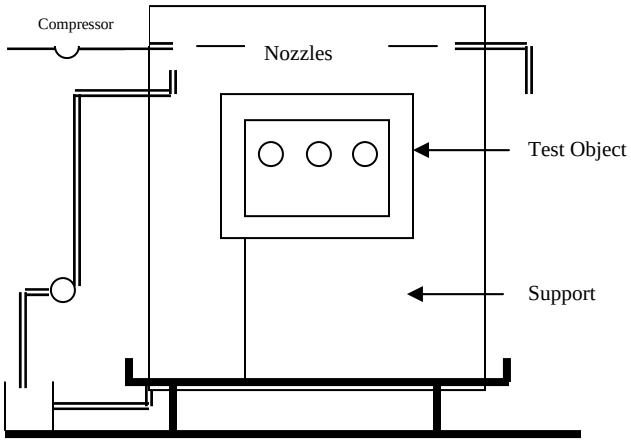

It was 160 *175*242 cm^3, contracted by plastic tube and covered by plastic sheets. Rainy condition was simulated by the help of pumps followed by compressed air. Three nozzles were provided at the corner of chamber and water recycled.

2.4 DISCHARGE MEASUREMENTS

To measure the discharges, ERA discharge detector had been used. It is basically a wide band amplifier with gain of 10^{-7} and band width of 10KHZ and thus provides resolution of 30μses.

2.5 DIELECTRIC LOSS MEASUREMENT

Dielectric loss and capacitances measurement were recorded by using Ratio Arm Bridge. It consists of a differential transformer with three winding W_1, W_2 and W_3. The test object and standard capacitor is connected in parallel and in series with two winding W_1 and W3 as shown in figure 2.

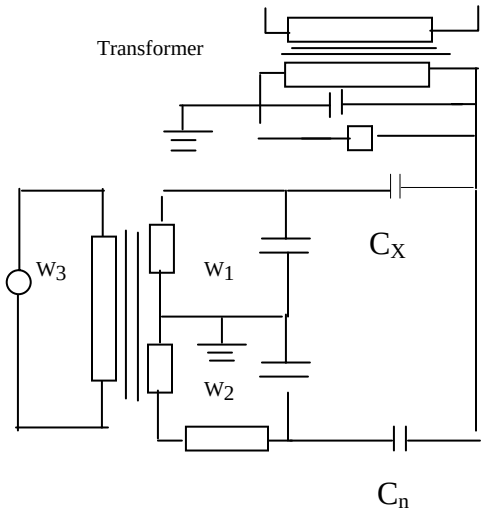

Figure 2: Dielectric loss and capacitance measurement circuit

Test object and standard capacitor is connected in parallel and in series with two winding W_1 and W_3. The connection point of W_1 and W_2 is grounded. The test voltage is applied to test object, standard capacitor and current i_1 and i_2 flows in the winding W_1 and W_2. The total induces flux will be zero when $W_1 i_1 = W_2 i_2$.If this condition not met then voltage will induced in and hence there is deflection and balance is obtained by variable taping winding W_2. In balanced condition, capacitance of the specimen C_x and Tanδ can be calculated as

$$C_x = C_n W_2 / W_1$$

Tanδ = $R^{/}$ ω $C^{/}$ Where $R^{/}$ is resistance for Tanδ balance and $C^{/}$ is capacitance decade for Tanδ balance composed of standard capacitance, stray capacitance, and cable capacitance.

2.6 Results and discussion

As mentioned earlier, measurement of partial discharges, Dielectric loss measurement, capacitance and discharge inception were recorded under dry, wet and contaminated conditions for every phase.

The measurements of above-mentioned parameters for each phase are slightly different but follow same pattern hence result of only one phases is presented for discussion. Dielectric loss shows increasing trend from dry to contaminated condition as shown Figure 3.

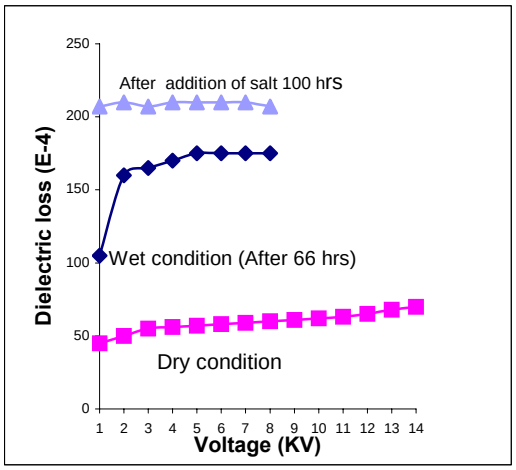

Fig. 3: Dielectric loss as function of voltage

Discharges starts earlier i.e. discharge inception voltage found less in contaminated condition compared with wet condition as shown in figure 4.

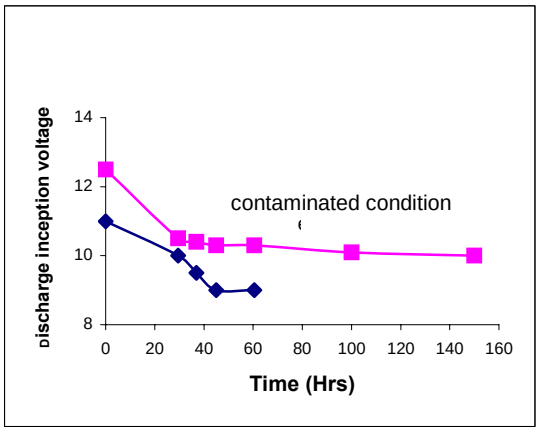

Fig. 4: Discharge inception voltage as a function of time

No appreciable change has been observed in capacitance in wet and contaminated conditions as shown in figure 5.

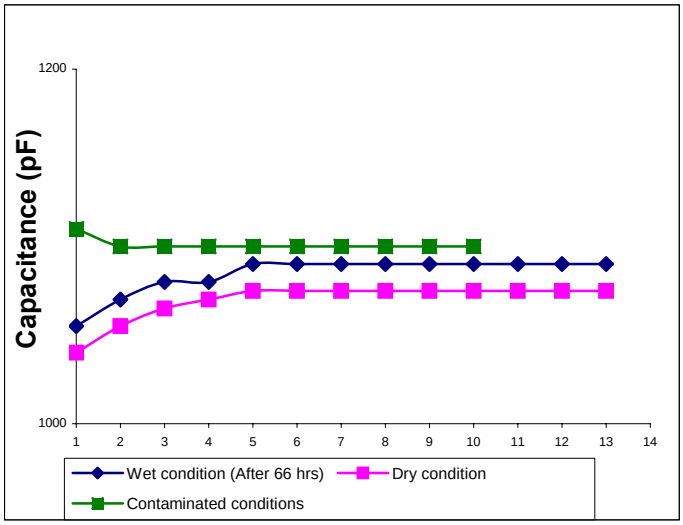

Fig. 5: Capacitance as a function of voltage

Dielectric loss/voltage under contaminated condition shows that characteristics have increased and changed from normal to rising characteristics. The curve which rises steady with voltage indicates the effect of contamination and deterioration of insulation. It is also observed that the knee point of the curve is very low. This gives an indication that discharge inception voltage is low.

When the termination is dry, a very small leakage current which is almost whole capacitive flows and voltage distribution is simply determine by the electrostatic field pattern. If however the surface become wet the pollution layer become conductive because of presence of ionic salt and surface leakage current flows in phase with applied voltage. This leakage current is generally many orders of magnitude greater than dry current, and so the electric filed is distorted to an extent which surface conductivity varies over entire insulator surface. The magnitude and distribution of pollution which may be deposited upon the termination can not be determined accurately because there are so many variable factor involved. However, some general conclusion can be drawn from the study of some processes considered in isolation. The conductivity of termination varies with time, and the dielectric loss increases as the contamination condition prolonged. The magnitude and distribution of fog depend upon

- **Gravitation force**
- **Pressure**

- **Electrical forces**

It is clear that the deposition of pollution increases with time and hence increases conductivity. Another possibility, which requires further investigation, is the effect of heating. Voltage is applied continuously so heating and evaporation is continuous. The formation of dry band and wet band follows over whole the termination. This gives a complicated variation of leakage current. This is one reason why the dielectric loss/voltage characteristics are not uniform.

The wet and contaminated condition is carried out over a relatively short time. Since the conductivity of salt is higher i.e. 6000 μs/cm and it has great effect on the dielectric loss and discharge inception voltage. It seems early aging of cable termination occurs.

After completing the experiment, the cable termination including the bushing was observed to check the effect of these tests on the surface insulation. No visible tracking was found nor carbon path or pitting in the bushing surface. So it can be predicated the deterioration occurred inside cable termination.

CONCLUSION

It has been derived from experiment that discharge inception voltage decreases, as we move from dry to wet and contaminated condition. Similarly dielectric loss and capacitance also increases. These results clearly describe the condition of the cable termination and it's aging. It can be concluded with confidence that deterioration and early aging occurred inside cable termination.

REFERENCES

1. **E Lemka H Elze and W .Weissenberg, Switzlang "Experience in dianossis tests of H.V cable termination in service using ultra wide band probing" XIIIth International symposium on High Voltage Engineering, Natherlands 2003.**
2. **M de Nigris G Rizzi, F.Pulletti TeachImp, A Cavallinni G.C Montanari M. Counti, University of Bologma Itely. "Cable Diagnossis based on defect location and characterization through partial discharge measurements" CIBRE 21 nue d Actos F-75008**
3. **Dr F.H KREUGER "Discharge detection in high voltage equipment" A Heywood book tample press 1984**
4. **K.KUFFEL AND W.S ZACHGL "High voltage engineering fundamentals" Perghmon press 1984**
5. **GOLDING "Electrical measurement and measurement instrument" Sir Isaac pitman & sons LTD London**

6. Judd, M.D. Farish, O. Pearson, J.S. Hampton, B.F Inst. for Energy & the Environinent, Strathclyde Univ., Glasgow.; "Dielecrtic windows for UHF discharge detection" IEEE Trans on electrical insulation, Dec 2001 valume 8, Issue 6

7. Boonseng, C.; Apiratikul, P.; Nakaviwat, K. "A high voltage cables terminator for partial discharge and dielectric loss measurement" Electrical Insulation, 2002. Conference Record of the 2002 IEEE International Symposium onVolume , Issue , 7-10 Apr 2002 Page(s): 62 – 65.